Theoretical Investigation of the Mechanism of the Selective Catalytic Reduction of Nitrogen Oxide with Ammonia on Fe-Form Zeolites

ARTICLE *in* THE JOURNAL OF PHYSICAL CHEMISTRY C · OCTOBER 2011

Impact Factor: 4.77 · DOI: 10.1021/jp206931z

THE JOURNAL OF PHYSICAL CHEMISTRY C

ARTICLE

pubs.acs.org/JPCC

Theoretical Investigation of the Mechanism of the Selective Catalytic Reduction of Nitrogen Oxide with Ammonia on Fe-Form Zeolites

T. C. Brüggemann* and F. J. Keil

Department of Chemical Engineering, Hamburg University of Technology, D-21073 Hamburg, Germany

Supporting Information

ABSTRACT: The selective catalytic reduction (SCR) of NO with NH_3 has been investigated on a portion of the Fe-ZSM5 which contains five T-atoms by using density functional theory. The iron was represented as a mononuclear species. For the fast SCR and NO_2 SCR, it is most likely that ammonia adsorbs on $Z^-[FeO]^+$ and a proton transfer leads to $Z^-[NH_2FeOH]^+$. A subsequent reaction with NO or NO_2 forms nitrosamine or nitramide together with $Z^-[FeOH]^+$, which is probably the most abundant surface species. The reduction of monohydroxylated iron with ammonia leads to $Z^-[FeNH_2]^+$ and water, and a final reaction of the amino group with NO_2 to nitrosamine restores the initial site. The intermediates nitrosamine and nitramide can be assumed to decompose on Brønsted acids to nitrogen and nitrous oxide, respectively, together with water. For the increase in selectivity of the NO_2 SCR to nitrogen with temperature, a decomposition of both intermediately formed N_2O and NO_2 to NO and oxygen was concluded to be responsible, rather than an additional high-temperature pathway. With respect to the decomposition of nitric acid on $Z^-[FeOH]^+$ to dihydroxylated iron and NO_2 followed by the reaction with ammonia to $Z^-[NH_2FeOH]^+$, a mechanistic explanation for the new "enhanced" SCR is also outlined. Finally, the reaction of oxygen with $Z^-[FeNH_2]^+$, leading first to the radical H_2NO and then via nitroxyl to NO, is capable to explain the mechanism of the selective oxidation of ammonia. The results of this work account for many observed phenomena of the experimental literature.

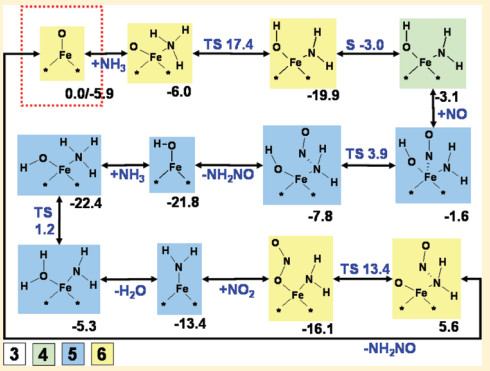

INTRODUCTION

The selective catalytic reduction (SCR) of nitrogen oxides with ammonia or hydrocarbons has become a key technology in the after-treatment of exhaust gases.[1,2] Besides the application in the production of nitric acid,[3] more stringent legislation for automobiles like the EURO IV and V[4] has led to an intensification of research in this field for diesel-engined vehicles. Several materials are known to be active for this reaction, but besides the established V_2O_5-containing catalysts, by now, metal-containing zeolites appear to be more favorable with respect to durability and activity.[5] Especially iron-exchanged ZSM5 has been in the focus of research over the last two decades.

Several groups[6−9] have examined this catalyst from different perspectives to understand its governing parameters, which are responsible for the activity as well as the mechanisms of its surface chemistry. Several studies concentrate on the impact of different techniques to introduce the metal into the zeolite, covering chemical vapor, liquid, and solid ion exchange methods or impregnation.[10−13] The resulting nature of the metal in the final catalyst and the corresponding activity of the exchanged species is also a key aspect of these studies. There is an agreement in the literature that, independent of the applied technique, potentially several different species coexist, emphasizing mono- and dinuclear iron sites, exchanged to the Brønsted acids of the parent H-form zeolite as well as Fe_xO_y iron clusters.[14,15] In most studies,[6,16−18] the iron species, resulting from a 1:1 exchange of the Brønsted acids[19] are believed to be the active species for the SCR. Kröcher et al.[20,21] recently stated based on a Poisson distribution analysis that the isolated sites are most relevant at low temperatures, while dinuclear iron sites significantly contribute to the reaction at elevated temperatures. Furthermore, the iron clusters are believed to be especially active for the unwanted oxidation of ammonia.[22,23] Finally, also the Brønsted acids are known to be active for the SCR,[24−31] and their contribution to the reaction remains under debate.[6,32−35]

Another key aspect of the investigation on the SCR is the underlying mechanism on the active sites with the intention to better understand the surface chemistry but also to develop kinetic models to simulate the reaction. This is of certain interest to optimize the operating parameters of exhaust gas treatment devices, including heat and mass transfer, but also to develop control devices for optimal ammonia dosage or NO oxidation in diesel oxidation catalysts (DOCs).[36,37] Several macroscopic phenomena are well established by now, including, besides the stoichiometry of the standard SCR (eq 1), also the boosting effect of NO_2[38−40] on the reaction, which exhibits a maximum in activity for the ratio of $NO_2/NO_x = 0.5$ and is known as the fast

Received: July 20, 2011
Revised: October 24, 2011
Published: October 24, 2011

SCR (eq 2).

$$4NH_3 + 4NO + O_2 \rightleftharpoons 4N_2 + 6H_2O \quad (1)$$

$$2NH_3 + NO + NO_2 \rightleftharpoons 2N_2 + 3H_2O \quad (2)$$

$$2NH_3 + 2NO_2 \rightleftharpoons N_2 + N_2O + H_2O \quad (3)$$

$$2NH_3 + 2NO + NH_4NO_3 \rightleftharpoons 3N_2 + 5H_2O \quad (4)$$

$$4NH_3 + 3O_2 \rightleftharpoons 2N_2 + 3H_2O \quad (5)$$

Further increase of this ratio finally leads to the pure NO_2 SCR (eq 3), which exhibits a slightly reduced activity as compared to the fast SCR, and a significant production of unwanted N_2O is observed. Because the production of nitrous oxide is strongly dependent on temperatures,[39−41] additional different stoichiometric equations are usually attributed with this reaction suggesting different underlying mechanisms.[37,42] The accepted explanation for the boosting effect of NO_2 on the SCR is the assumption that in the standard SCR the oxidation of NO to NO_2 is required and the rate-determining step.[39,39,43−45] With that, the fast SCR can be interpreted to be the true SCR.[46] However, a discrepancy in this explanation is devoted to the fact that water, which is produced in the SCR, strongly inhibits the NO oxidation,[39,41,45,47] and Fe-ZSM5 was found to be significantly less active for this reaction than for the SCR. Delahay et al.[43] suggested that the rate-limiting step of the NO oxidation should be the desorption of NO_2 from the catalyst and that in the SCR this step is circumvented because ammonia directly reacts with the adsorbed species. Similarly, Metkar et al.[45] recently suggested the formation of adsorbed nitrous and nitric acid in the presence of water, which are blocking the NO oxidation. Ammonia is then assumed to react with the acids and, thus, to remove these limiting agents. Nevertheless, the fact that Metkar et al. found similar activities for the SCR and the NO oxidation in the absence of water is in disagreement with Delahay et al.[43] and Schwidder et al.,[8] who found significantly lower activities for the oxidation. Recently, we have outlined that the inhibiting influence of water on the NO oxidation is related to a change of the active site from FeO to FeOH.[48] Furthermore, nitrous and nitric acid were shown to either decompose into an adsorbed hydroxyl group together with NO_x or form a surface nitrite or nitrate, respectively, and are, thus, not expected to remain adsorbed, as stable molecules, on the mononuclear iron sites. With respect to an observed inhibition of the SCR by ammonia,[49,50] another explanation for the reduced activity of the standard SCR vs the fast SCR is related to a blocking of the active site for the NO oxidation.[37,45,51,52] Thus, for the connection between the fast SCR and the standard SCR, a severe interest in the elucidation of the detailed mechanism remains.

Furthermore, Tronconi et al.[53,54] have established a new reaction system including ammonium nitrate (or nitric acid) as the additional reducing agent besides ammonia for the SCR (eq 4). They observed a significant enhancement of the SCR, compared to the standard case, but not as pronounced as for the fast SCR. They related the increase in activity to their suggestion that ammonium nitrate is an essential intermediate of the fast SCR. Also, the oxidation of ammonia (SCO) (eq 5) was found to be active on Fe/H-ZSM5,[55−57] especially at elevated temperatures, and Yang et al.[58−60] observed a correlation between the SCO selectivity toward nitrogen and the SCR activity. Finally, the decomposition of nitrous oxide, as investigated in detail by Heyden et al.,[61−63] and the SCR of nitrous oxide, as studied by Coq et al.[64−67] and other authors,[68,69] have to be mentioned as part of the complex system of reactions within the SCR as well.

The mechanistic explanation for the standard, fast, and NO_2 SCR is dominated by Tronconi et al.[42,70,71] who proposed a sequence of reactions for iron zeolites in analogy to Koebel et al.[72,73] for a vanadium-based catalyst. A similar mechanism was stated for a BaNa−Y catalyst by Weitz et al.[74,75] The key steps which are claimed to be valid also for V_2O_5 and Cu-zeolites involve the disproportionation of two NO_2, leading eventually to ammonium nitrite and nitrate which decompose to nitrogen and nitrous oxide. The rate-determining step in the fast SCR is claimed to be the reaction of NO with a nitrate species to nitrite. The nitrate and nitrite species are also sometimes written in terms of nitric and nitrous acid, involving water in the disproportionation sequence of NO_2.[7,40] However, the mechanism neglects a discrimination of the coexistence and activity of different active sites and, thus, keeps a rather macroscopic and speculative character despite the formulation of a potential intermediate.

A detailed analysis of the elementary steps within the reactive system of the SCR on iron as the active site that is capable to explain the macroscopically observed phenomena has so far only been attempted to a small extent by Li and Li.[76] Such a study could help to better understand the mechanisms of the single systems and their interaction and serve not at last as a basis for the development of more sophisticated rate expressions for reactor simulations. Nevertheless, tracing surface chemistry to the elementary steps is only possible with theoretical methods like DFT. In our previous study,[48] we have analyzed the oxidation of NO on mononuclear iron sites in the absence and presence of water and could explain the difference in activity with respect to a change of the structure of the active site from FeO to FeOH. Also, the key surface species mono- and dihydroxylated iron as well as surface nitrite and nitrate were identified. The choice of the mononuclear species was related to results from Kröcher et al.[20,21] who suggested these species to be most active in the economically favored low-temperature regime, and also Grünert et al.[8,18,77] claimed isolated iron sites to be the active species in the SCR. The goal of this work, in continuation of our previous study, is to establish a reaction network for mainly the fast and the NO_2 SCR that accounts for the experimentally observed phenomena on mononuclear iron sites. The varying stoichiometry and selectivity of the NO_2 SCR with respect to nitrous oxide is discussed. In addition, the impact of oxygen on ammonia is presented allowing for suggestions on the mechanism of the SCO. Following our investigations of the H/N/O system on the Brønsted acids as the active site,[24,25,78] the main intermediate gas-phase species are assumed to be nitrous and nitric acid as well as nitrosamine and nitramide within the SCR and nitroxyl and hydroxylamine in the SCO. Because from microkinetic modeling[79] the decomposition of the intermediates nitrosamine and nitramide to nitrogen and nitrous oxide, respectively, was found to be very fast on the Brønsted acids, we assumed this pathway to be dominating also in the Fe/H-ZSM5. Thus, the here described catalytic cycles on the mononuclear iron sites only cover the production of these key intermediates. However, together with our previous results on the NO oxidation,[48] a detailed description of the mechanisms in the SCR based on mononuclear iron sites is outlined.

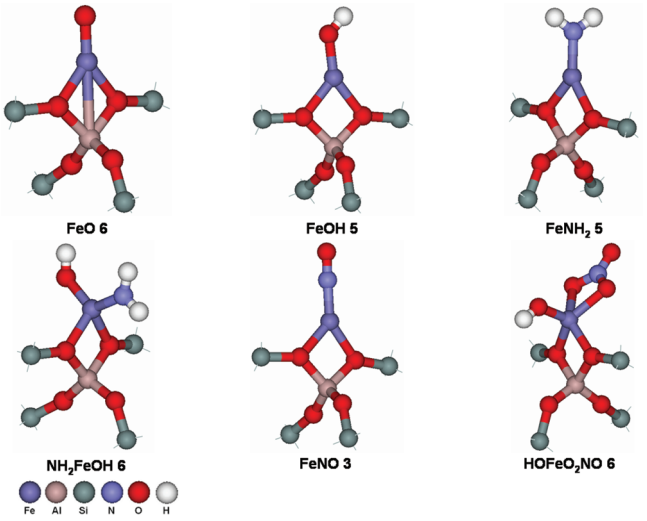

Figure 1. T5 cluster model of the significant intermediates of Fe-ZSM5: $Z^-[FeO]^+$, $Z^-[FeOH]^+$, $Z^-[FeNH_2]^+$, $Z^-[NH_2FeOH]^+$, $Z^-[FeNO]^+$, and $Z^-[HOFeO_2NO]^+$. The numbers correspond to the spin multiplicity of the minimized species. Dangling bonds are not shown.

THEORY

The catalytic active center and a part of the zeolite framework were represented by a cluster of five T-sites (Figure 1, FeO), and all Si atoms were initially placed at their crystallographic positions, as reported by Olson et al.[80] The terminal Si atoms were saturated with hydrogen. The iron was considered as mononuclear ions, which replace the Brønsted acid site of the parent H-ZSM5. All quantum chemical calculations were carried out on potential energy surfaces (PES) with spin multiplicities M_S = 2−8, by using the gradient-corrected Density Functional Theory (DFT) as implemented in the TURBOMOLE suite of programs[81] at the B3LYP/TZVP level of theory with a very fine numerical grid size (m5).[82] Structure optimizations were performed in Cartesian coordinates with an energy convergence criterion of 10^{-7} Hartree, and the maximum norm of the Cartesian gradient was converged to 10^{-4} Hartree/bohr. Variations in the choice of the T-site for the aluminum in the zeolite framework as well as in the size of the representation of the catalyst were shown to have little impact on the results.[48] The specifications chosen in this work are considered as a reasonable compromise between accuracy and computational expenses.

Transition states were localized from a combined application of, first, the growing string method[83] and a refinement with either the modified dimer method[84] with a gradient norm convergence criterion of 5×10^{-4} Hartree/bohr or the PRFO[85] method. Minimizations of the surface species on different PESs revealed that the energy differences between them are usually significant such that only the ground state needs to be considered. However, in cases with two PESs being close to each other, we also considered the crossing of PESs to obtain the lowest energy pathway for the overall catalytic cycle. For the excited states, we then considered only the state of lowest energy. In iron core containing systems, the B3LYP functional gives results for relative energies between the ground and the lowest excited state which are in most cases in good agreement with high-level ab initio quantum mechanical calculations.[86−88] Crossing of seams of PESs in minimu energy crossing points (MECPs) were determined with a multiplier penalty function algorithm which had a maximum energy difference on both PESs of less than 10^{-6} Hartree. To calculate Gibbs' free energies also for the MECPs, we calculated the vibrational frequencies for the partition function based on an effective Hessian as stated by Harvey and Aschi.[89] Energy barriers obtained from transition state search as well as MECPs have limited accuracy and are dependent on the applied density functional.[90−92] However, based on the successful application to the investigation of the decomposition of nitrous oxide in Fe-ZSM5 in our institute[61−63] and by Guesmi et al.,[93] which lead in both cases to even quantitative agreement with experiments,[94−96] it can be assumed that the accuracy of the methodology applied here is sufficient for at least a qualitative analysis of the SCR on Fe-ZSM5.

RESULTS AND DISCUSSION

The mechanism of the selective catalytic reduction of NO with ammonia can mainly be subdivided into the macroscopic reactions: NO oxidation, the fast SCR, the NO_2 SCR, the ammonia oxidation, and the decomposition of nitrous oxide. The NO oxidation was already discussed by Brüggemann and Keil[48] and the decomposition of N_2O investigated in detail by Heyden et al.[62,63,97] Here, the main focus is set on the fast and the NO_2 SCR according to the equations (eq 2 and eq 3) with some additional remarks on the ammonia oxidation and the crossover to the nitrous oxide decomposition. On the basis of our previous results[48] on the NO oxidation which suggested FeO and FeOH to be the representations of the active sites, we neglect other surface species as the starting point of a catalytic cycle. In fact, because hydrogen is introduced into the system by ammonia, a clear differentiation between the active site structure, as was done for the NO oxidation, is not possible here. In addition, the interaction of ammonia with the as stable concluded dihydroxylated iron and iron nitrite will be discussed in the context of their appearance in the considered catalytic cycles. In a similar study on the SCR on the H-form zeolite,[24,25,79] we have shown that Brønsted acids are very active for the decomposition of the intermediates nitrosamine and nitramide into nitrogen and nitrous oxide, respectively, together with water. We have assumed that these species are also essential intermediates in the catalytic cycle on iron as the active site and that their decomposition takes place on the acid sites also in the presence of iron. The decomposition on the iron cannot be ruled out, but within this work, the impact of such an analysis is believed to be negligible. Furthermore, we have shown that nitrous and nitric acids are produced on the Brønsted acids within the fast SCR but also within the NO oxidation in the presence of water on the iron sites. Thus, we also consider their potential interaction with ammonia on the Fe-ZSM5. Finally, for the oxidation of ammonia on the Brønsted acids, the key intermediates were suggested, based on DFT, to be nitroxyl and hydroxylamine,[78] and their potential production and consumption on iron sites will be discussed within the framework of the SCR.

The following discussion will be subdivided into four parts. In the first part, we focus on the mechanism of the fast SCR. In the second part, the mechanism of the NO_2 SCR will be covered with respect to the experimental finding of a temperature-dependent selectivity of the nitrogen vs nitrous oxide production. In the third part, we analyze the influence of oxygen on the system other than the NO oxidation. Finally, in the fourth part, aspects of the ammonia oxidation as well as the interaction with the N_2O decomposition will be discussed. As part of the investigations,

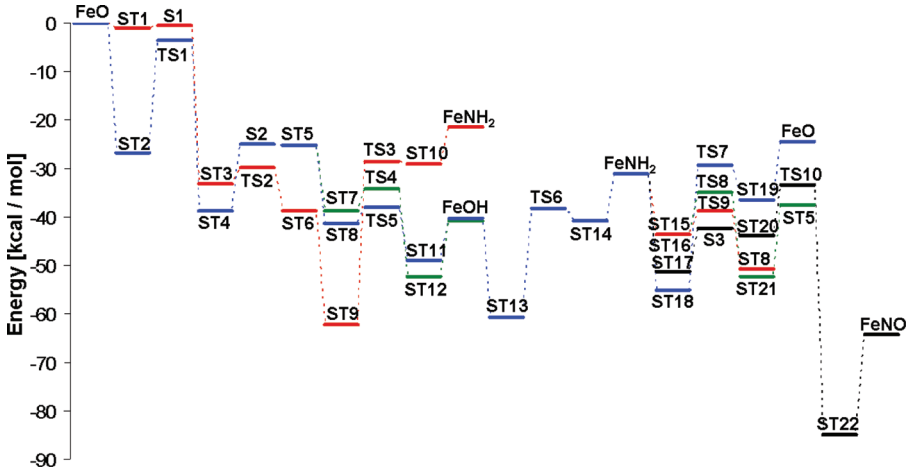

Figure 2. Energy profiles for the catalytic cycles of "part one: the fast SCR" on $Z^{-}[FeO]^{+}$. Energies are zero-point corrected.

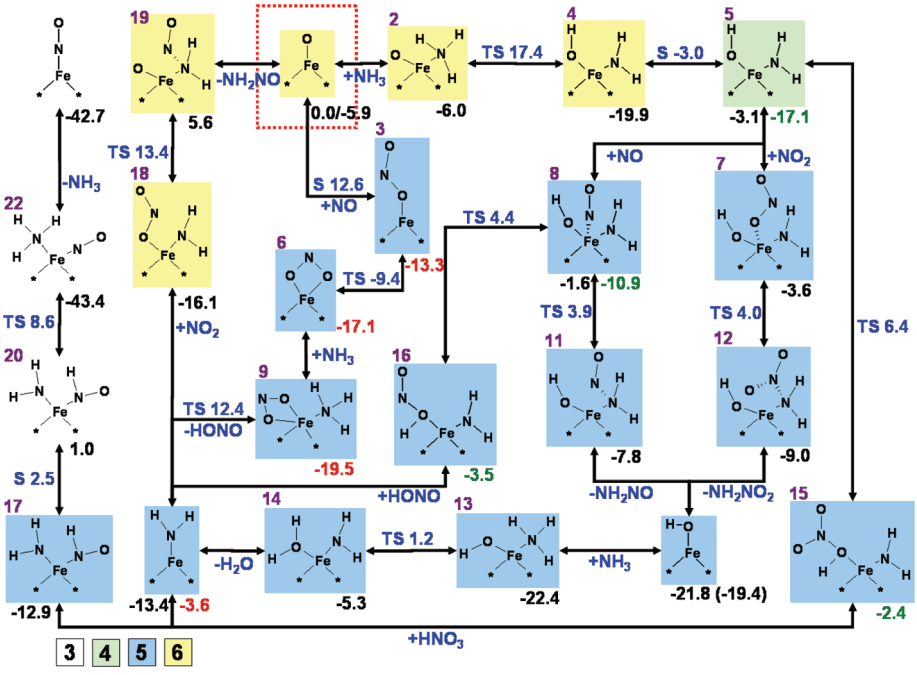

Figure 3. Overview of considered catalytic cycles of "part one: the fast SCR" on $Z^{-}[FeO]^{+}$. Stated values are Gibbs' free energies calculated at 600 K. Purple numbers refer to the structure labels of Figure 2. Black numbers correspond to the structure and blue numbers to the transition states (TS) or to the minimum on the seam of two PESs (S). The second value below $Z^{-}[FeO]^{+}$ corresponds to the closed reaction cycle. Red numbers refer to the alternative pathway via $Z^{-}[FeO_2N]^{+}$, and green numbers refer to the decomposition of nitrous or nitric acid on $Z^{-}[FeNH_2]^{+}$. Colors of the boxes correspond to the spin multiplicity.

we also considered the crossing of potential energy surfaces of different spin multiplicities, to account for the different spin states of overall reactants and products as well as to find the minimum energy pathway (MEP) for the catalytic cycle. The labeling of the structures involved naming the ligands to the iron. In the case that three ligands have been considered, one of them is annotated with a minus ("−"). In the case that a molecule is considered as a gas phase species, we used an underline character ("_") to add it to the tag. For all parts, the mechanistic overviews and the energy diagrams of the different catalytic cycles are provided. All the energies in the diagrams are zero-point energy-corrected, and the values in the overviews are Gibbs' free energies calculated at 600 K. The black values refer to the structures and the blue values to either transition states or the barrier for the crossing of a seam between two PESs. The colors of the boxes refer to the spin multiplicity of the PES as follows: purple refers to $M_S = 2$, white to $M_S = 3$, green to $M_S = 4$, blue to $M_S = 5$, yellow to $M_S = 6$, and orange to $M_S = 7$. In both, energy diagram and overview, the values are given with respect to FeO as the active site structure (if not stated differently) and gas phase molecules as reference. The value of 600 K was picked to consider the entropic effects of the reaction mechanism at a temperature at which also the standard SCR with ammonia shows significant conversions.

dx.doi.org/10.1021/jp206931z |J. Phys. Chem. C 2011, 115, 23854–23870

With respect to the limited accuracy of the DFT in general and to the calculation of energy barriers from transition states and minimum energy crossing points, it should be emphasized that all the subsequently presented results are of qualitative nature only.

Part 1: The Fast SCR. In this part, mainly the catalytic cycle of the fast SCR is discussed with FeO (Figure 1) in its ground state on the PES with $M_S = 6$ as the reference structure. The energies are shown in Figure 2, and the schematic overview of the reactions, including the Gibbs' free energies at 600 K, is shown in Figure 3. The corresponding structures of the species are shown in Figure S1 in the Supporting Information. The adsorption of ammonia on this structure was found to exhibit a rather high energy of adsorption of $\Delta E_{ads} = -26.8$ kcal/mol (ST 2) with the ammonia attached to the iron by its nitrogen atom and a hydrogen bond to one of the zeolite framework oxygens. Then, a proton transfer takes place from the adsorbed ammonia to the oxygen leading to an amino group together with a hydroxyl group (ST 4). This step exhibits an energy barrier of $E^{\ddagger} = 23.3$ kcal/mol (TS 1) and is exothermic by $\Delta E = -12.0$ kcal/mol. Thus, for the observable adsorbed state of ammonia on the iron, two different species (ST 2 and ST 4) have to be taken into account with a resulting heat of adsorption for ST 4 of $\Delta E_{ads} = -38.7$ kcal/mol. The species so far were calculated on the sextet PES. However, the subsequent reactions with either NO or NO_2 were found to proceed on the quintet PES, which requires, at this stage, a crossing from the ground state sextet to the quartet (ST 5) PES via S2 and a barrier of $E^{\ddagger} = 13.7$ kcal/mol (electronic energy only). The adsorption of NO to this species with the nitrogen bonded to the iron (ST 8) is only weak with respect to the prior ground state. Nevertheless, a subsequent reaction via the TS 5 with a low barrier of $E^{\ddagger} = 3.4$ kcal/mol leads to the formation of nitrosamine, adsorbed on monohydroxylated iron (ST 11). Finally, the desorption of NH_2NO with a heat of desorption of $\Delta E_{des} = 8.5$ kcal/mol leads to the ground state FeOH on the quintet PES. Overall, this first formation of nitrosamine was calculated to be exothermic by $\Delta E = -40.3$ kcal/mol. It is at hand that the equilibrium conditions between the ground and the excited state of the intermediate NH_2FeOH dictate only rather small quantities of the quartet species to be available on the catalyst. However, the fact that the ground state is rather stable and the gap between the two states is sufficiently small makes the assumption of the excited state to be present reasonable. Furthermore, the subsequent reaction with NO has to be considered as being fast because of the rather low barrier, and thus, this pathway can be concluded to be accessible. Alternatively, also NO_2 can coadsorb on the excited state of NH_2FeOH, although here the nitrogen dioxide is only hydrogen bonded to the amino group (ST 7). A subsequent reaction in analogy to the formation of nitrosamine results in nitramide adsorbed on the monohydroxylated iron (ST 12) by overcoming a barrier of $E^{\ddagger} = 4.6$ kcal/mol (TS 4). The desorption of NH_2NO_2 with $\Delta E_{des} = 11.4$ kcal/mol eventually leads to FeOH. In a next step, ammonia adsorbs on the monohydroxylated iron with, again, the nitrogen bonded to the iron and a hydrogen bond to a framework oxygen with a heat of adsorption of $\Delta E_{ads} = -20.3$ kcal/mol. Similar to TS 1, another proton transfer from the ammonia to the hydroxyl group takes place, forming water coadsorbed to an amino group (ST 14). This step exhibits an activation energy of $E^{\ddagger} = 22.2$ kcal/mol and is in magnitude quite close to the prior proton transfer corresponding to TS 1. Then, water desorbs with $\Delta E_{des} = 9.6$ kcal/mol and leaves iron with an amino group on the quintet PES, denoted as $FeNH_2$ (Figure 1). To complete the catalytic cycle of the fast SCR, the adsorption of NO_2 to this species is required, which is strongly bonded to the iron by one oxygen (ST 18, $\Delta E_{ads} = -24.1$ kcal/mol) on the PES with spin multiplicity $M_S = 6$. The subsequent reaction via TS 7 leads to the formation of nitrosamine adsorbed on the initial active site FeO (ST 19) and exhibits a high barrier of $E^{\ddagger} = 25.8$ kcal/mol. Finally, the desorption of NH_2NO with $\Delta E_{des} = 12.1$ kcal/mol restores the initial active site FeO. Although the second formation of nitrosamine requires us to overcome the highest internal barrier of the complete cycle with TS 7 and is endothermic by $\Delta E = 30.7$ kcal/mol (FeO − ST 18), it has to be pointed out that the species NH_2FeONO has to be considered quite stable, while the products nitrosamine and FeO are rapidly consumed. Thus, the equilibrium of this final elementary step will always be dragged to the product site.

Tronconi et al.[42,70,71] have suggested that the rate-limiting step in the fast SCR should be the reduction of a surface nitrate with nitric oxide to a surface nitrite. Brüggemann and Keil[48] have recently shown that such a step exhibits a barrier of $E^{\ddagger} = 35.7$ kcal/mol, which is nearly 10 kcal/mol higher than the highest internal barrier in our pathway. Despite the fact that this result does not allow for a conclusion on the mechanism on iron species of higher nuclearity, for the mononuclear iron sites it clearly indicates that the reaction proceeds via the amino groups rather than the nitrates. From the energy profile (Figure 2), it has to be noted that FeOH marks a valley in the catalytic cycle and from this perspective can be assumed to be the dominating surface species. The potential formation of nitramide, from the reaction of NO_2 with NH_2FeOH instead of NO, depicts in the final catalytic cycle the NO_2 SCR with the stoichiometry of reaction (eq 3). Because nitramide decomposes to nitrous oxide on the Brønsted acids, this pathway can be seen as the explanation of the high production of N_2O within the NO_2 SCR at low temperatures.

Alternatively, we also considered the adsorption of NO on FeO together with a spin change from the septet to the quintet PES (S1) leading to an iron nitrite (ST 3) that is bonded with one oxygen to the iron. A low barrier reaction (TS 2) leads then to the more stable nitrite with two oxygen atoms bonded to the iron (ST 6). This was already outlined in the context of the NO oxidation.[48] Next, ammonia strongly coadsorbs to the nitrite with $\Delta E_{ads} = -23.6$ kcal/mol (ST 9). A hydrogen transfer from the ammonia to the adsorbed nitrite results in the formation of nitrous acid. The latter remains only hydrogen bonded to the formed amino group on the iron (ST 10) and finally desorbs with $\Delta E_{des} = 7.7$ kcal/mol. The formation of the acid, however, requires overcoming a barrier of $E^{\ddagger} = 33.8$ kcal/mol (TS 3), which is significantly higher than the highest barrier of the formerly discussed pathway. Nevertheless, the exothermicity of the formation of the nitrite and the strong coadsorption of ammonia suggest the formation of ST 9 in reasonable quantities on the catalyst. With that, this pathway cannot be ruled out. However, the analogous reaction of water with the nitrite revealed a barrier of only $E^{\ddagger} = 22.6$ kcal/mol leading to FeOH.[48] Thus, in the presence of sufficient amounts of water, nitrous acid will be produced from the reaction of water with the surface nitrite rather than with ammonia. In transient experiments and in the absence of water, the reaction with ammonia might dominate. An analogous transition state for the reaction of ammonia with FeO_2NO to nitric acid and the $FeNH_2$ was not found. However, for the reaction of water with the nitrate, we found a barrier of $E^{\ddagger} = 26.9$ kcal/mol which is slightly higher than the corresponding

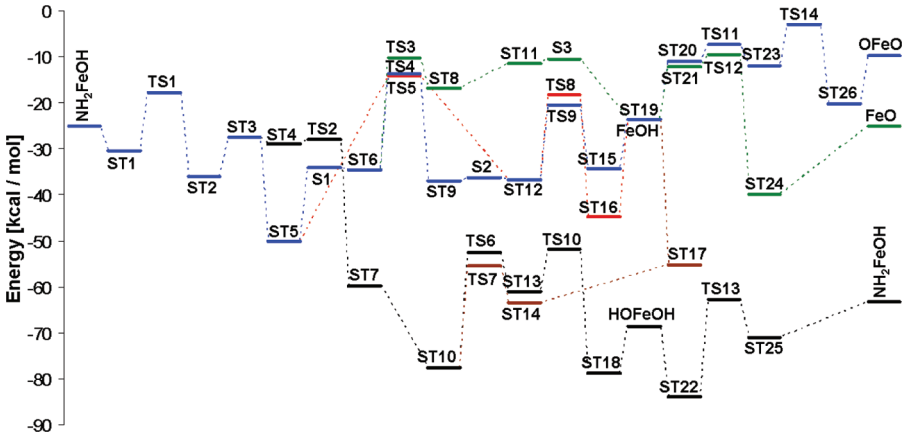

Figure 4. Energy profiles for the catalytic cycles of "part two: the NO_2 SCR" on $Z^-[FeO]^+$. Energies are zero-point corrected.

reaction with the nitrite. With respect to the structural similarity of the transition structures for the reaction of the nitrite with either water or ammonia and the reaction of water with the nitrate, it can be assumed that a barrier for the reaction of ammonia with the nitrate should also be slightly higher than the corresponding reaction with the nitrite.

In the main pathway, $FeNH_2$ can be interpreted to be a key intermediate, and we also considered the interaction of nitrous and nitric acid with this species. Both acids adsorb to it with a bond of the oxygen of the hydroxyl group to the iron and with a hydrogen bond to the zeolite framework (ST 15: nitric acid; ST 16: nitrous acid) with similar heats of adsorption $\Delta E_{ads} = -12.4$ kcal/mol and $\Delta E_{ads} = -12.5$ kcal/mol, respectively. Then, via TS 8 and TS 9 the bond between the hydroxyl group of the acid and the corresponding NO_x is broken, and NO_2 and NO are released. This step exhibits activation energies of $E^{\ddagger} = 8.5$ kcal/mol and $E^{\ddagger} = 4.8$ kcal/mol. In the case of the nitric acid, the released NO_2 only remains hydrogen-bonded to the hydroxyl group (ST 21); however, for the nitrous acid decomposition, the NO forms a bond with the nitrogen to the iron, and the species is analogous to ST 8 of the main cycle. From a mechanistic aspect as well as with respect to the energy barriers, the decomposition strongly resembles the decomposition of the acids on monohydroxylated iron, eventually leading to dihydroxylated iron.[48]

Finally, we also include in this context the interaction of nitroxyl with $FeNH_2$ which was shown on the H-ZSM5 to be a significant intermediate from the oxidation of ammonia and is expected to be relevant also on iron-containing zeolites. HNO strongly adsorbs with the nitrogen bonding to the iron with $\Delta E_{ads} = -20.1$ kcal/mol (ST 17). Then, prior to a hydrogen transfer from the nitroxyl to the amino group, a spin change from $M_S = 5$ to $M_S = 3$ (ST 20) is required because the final product state (ST 22) has its ground state on the triplet PES, and the hydrogen transfer was found to proceed with a slightly lower barrier on this PES. This step exhibits a barrier of $E^{\ddagger} = 8.9$ kcal/mol (S 3, electronic energy only). For the hydrogen transfer, leading to ammonia adsorbed on FeNO (ST 22), a barrier of $E^{\ddagger} = 10.5$ kcal/mol (TS 10) was calculated. Because this step is highly exothermic by $\Delta E = -41.1$ kcal/mol and the two preceding barriers are sufficiently low, it can be assumed that nitroxyl reacts rather fast with the $FeNH_2$ intermediate, reforming ammonia.

From the Gibbs' free energies in Figure 3, it can be seen, in agreement with the above discussion, that the pathway of the fast SCR via first the ammonia adsorption is in favor over the reaction of ammonia with the nitrite because of the lower overall energy barriers. Also the very stable character of the intermediate FeOH can be observed from the low Gibbs' free energy supporting the suggestion of this species to be dominant on the surface. Finally, the importance of the formation of FeNO from the reaction of nitroxyl with the amino group on the iron is supported by the extremely low energy values. Its accessibility is however anchored to the presence of $FeNH_2$ species in sufficient amounts.

Part 2: The NO_2 SCR. In part one, in the context of the fast SCR, we have outlined a potential mechanism of the NO_2 SCR leading to equimolar amounts of nitrogen and nitrous oxide. From the experimental literature it is known that the selectivity of this side reaction toward nitrogen is strongly dependent on temperature[39,40,42] with a maximum between 250 and 300 °C. Up to the maximum, indeed approximately equimolar amounts of nitrogen and nitrous oxide are observed, while at higher temperatures the selectivity drastically shifts toward nitrogen. Tronoconi et al.[42] explained this behavior from first the decomposition of ammonium nitrate to nitrous oxide at low temperatures. Then a reaction of ammonia with surface nitrates as an additional NO_2 SCR mechanism to only nitrogen is suggested to set in at elevated temperatures. Finally, at high temperatures the partial decomposition of NO_2 into NO and oxygen is proposed to make the fast SCR accessible. Also, Chatterjee et al.[98] and Schuler et al.[36] assumed different reactions for the NO_2 SCR, within the kinetic modeling of the SCR, to account for the observed change in selectivity. Thus, we probed the PES with respect to an additional pathway only resulting in the production of nitrogen to discuss the potential accessibility to different mechanisms. Furthermore, a strict differentiation between the subreactions is not reasonable because of the crossings of the mechanisms, and thus also the interaction with NO will be discussed in this context. The energies of the reactions are shown in Figure 4, and an overview with the Gibbs' free energies at 600 K is shown in Figure 5. The structures of all species are shown in Figure S2 in the Supporting Information.

We start the discussion of the mechanism with the species NH_2FeOH (section eq 5, ST 5) on the quartet PES. Besides the interaction with NO_2 leading to nitramide as outlined in the preceding section, nitrogen dioxide can also adsorb to this species with an oxygen bonded to the iron (ST 1). However, it has to be pointed out that this adsorbed state is energetically less favorable than the hydrogen bonding to the amino group by

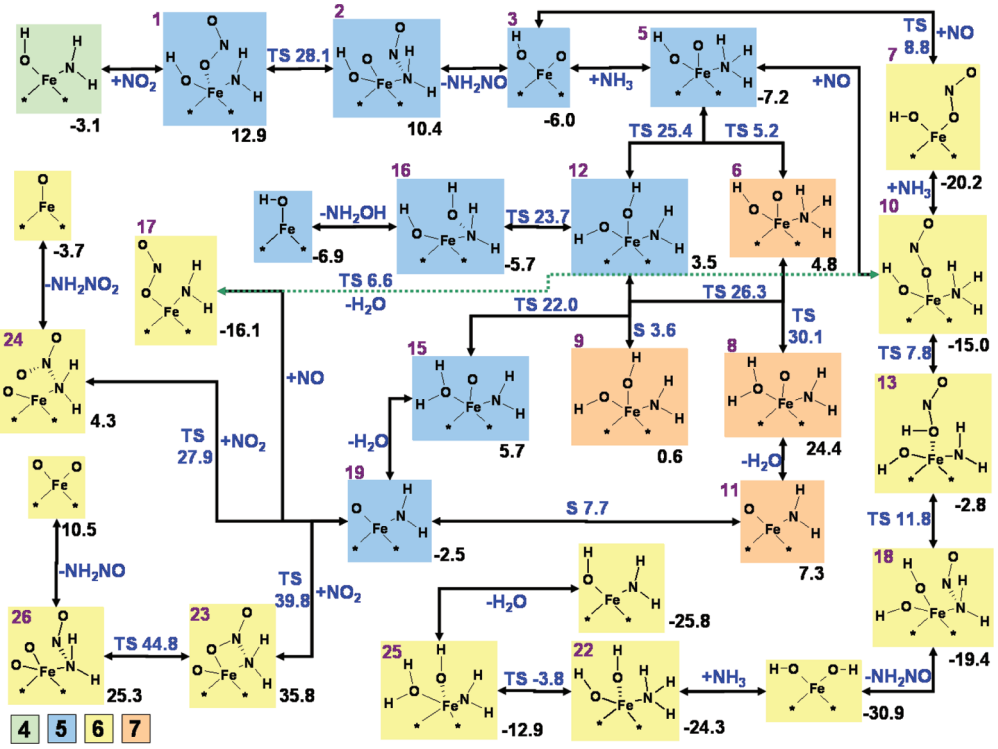

Figure 5. Overview of considered catalytic cycles of "part two: the NO_2 SCR" on $Z^-[FeO]^+$. Stated values are Gibbs' free energies calculated at 600 K. Purple numbers refer to the structure labels of Figure 4. Black numbers correspond to the structure and blue numbers to the transition states (TS) or to the minimum on the seam of two PESs (S). Colors of the boxes correspond to the spin multiplicity.

ΔE = 8.3 kcal/mol. In the subsequent reaction, the N−O bond in the adsorbed NO_2 is broken, and nitrosamine forms, adsorbed on OFeOH (ST 2). This step requires overcoming a barrier of $E^{\ddagger}$ = 12.8 kcal/mol (TS 1). Although this barrier is sufficiently low to be surpassed in comparison to the highest barrier of the fast SCR, compared to the competing reaction to nitramide ($E^{\ddagger}$ = 4.6 kcal/mol), this step is less favorable. Nevertheless, nitrosamine easily desorbs with ΔE_{des} = 8.5 kcal/mol, leaving OFeOH (ST 3) on the quintet PES. Ammonia adsorbs strongly to this species with ΔE_{ads} = −22.7 kcal/mol (ST 5) with its nitrogen bonded to the iron. For a subsequent transfer of a proton eventually leading to the formation of water, different scenarios were analyzed. For the most straightforward transfer from the ammonia to the hydroxyl group, only on the septet PES a transition state was found. This requires the spin change of the NH_3−OFeOH intermediate from its quintet ground state to the excited septet state (ST 6). The barrier for this process was calculated to be $E^{\ddagger}$ = 16.1 kcal/mol (S 1, electronic energy only). The proton transfer via TS 3 exhibits a barrier of $E^{\ddagger}$ = 24.4 kcal/mol leading to water, adsorbed on NH_2FeO (ST 8) on the septet PES. Because the initial spin change exhibits only a negligible barrier for the reverse reaction to the ground state, the hydrogen transfer should rather be seen as a combined step, involving the crossing of the seam S 1 together with the transition state TS 3. This combined step exhibits a barrier of $E^{\ddagger}$ = 40.0 kcal/mol and is endothermic by ΔE = 33.4 kcal/mol. Therefore, this step is rather unlikely to occur. A subsequent desorption of water (ST 11) and a recrossing to the ground state quintet PES via S 3 to NH_2FeO (ST 19) however only require overcoming a combined barrier of $E^{\ddagger}$ = 6.3 kcal/mol. Alternatively, starting from the excited state ST 6 a slightly lower barrier of $E^{\ddagger}$ = 20.9 kcal/mol (with respect to the ground state $E^{\ddagger}$ = 36.6 kcal/mol, TS 4) results in a proton transfer to the oxygen, bonded to the iron, forming a second hydroxyl group. Here, the septet PES corresponds to the ground state of this intermediate (ST 9), and though also this elementary step is endothermic, the product state is by ΔE = −20.3 kcal/mol lower in energy than ST 8. Finally, the proton transfer from the ammonia to the free oxygen was also determined on the quintet PES. The barrier for this step was calculated to be $E^{\ddagger}$ = 36.0 kcal/mol (TS 5), which is nearly the same value as on the septet PES. The resulting intermediate NH_2−HOFeOH on the quintet PES (ST 12) is only by ΔE = 0.2 kcal/mol higher in energy than the corresponding ground state (ST 9), and thus, with respect to accuracy of DFT, it cannot be concluded on which PES the true ground state is located. Nevertheless, the barrier from the septet to the quintet PES is negligibly small with $E^{\ddagger}$ = 0.8 kcal/mol. Finally, a proton transfer between the hydroxyl groups was considered which, on the quintet PES, requires overcoming a barrier of $E^{\ddagger}$ = 16.4 kcal/mol, (TS 9) leading, after the desorption of water, to the ground state of NH_2FeO (ST 19). From the energy profile (Figure 4), it can be concluded that the formation of water from ammonia and the hydroxyl group of OFeOH is severely more favorable via the intermediate formation of two hydroxyl groups. Although it cannot be excluded that the direct protonation occurs on the quintet PES with a lower barrier, from the prior results it is not expected to be significantly lower than TS 3 to TS 5. Thus, the significance of the interaction of ammonia with the intermediate OFeOH is questionable with respect to the rather high internal barriers.

Besides the final proton transfer between the hydroxyl groups on the quintet PES, the formation of hydroxylamine was considered from the amino group and one of the hydroxyl groups as

well. Hydroxylamine was found to be a significant intermediate in the SCO on the Brønsted acids,[78] and thus, this reaction step can be seen as a slight excursion with respect to the ammonia oxidation on iron. NH_2OH is formed on the iron via the transition state TS 8 ($E^{\ddagger}$ = 18.7 kcal/mol) and remains strongly adsorbed on the essential monohydroxylated iron (FeOH) with ΔE_{ads} = −21.2 kcal/mol (ST 16). Thus, the reverse route, starting from FeOH, involving the decomposition of hydroxylamine via TS 8 to ST 12 and the subsequent formation of water via TS 9 to ST 15 could be of importance in the SCO.

In the energy diagram, ST 17 reflects the species NH_2FeONO on the sextet PES, which forms from the strong adsorption of NO on the oxygen of NH_2FeO (ST19) with ΔE_{ads} = −31.7 kcal/mol. This species was shown in part one to further react to nitrosamine and FeO. In contrast, the interaction of NO_2 with ST 19, to complete the catalytic cycle of the NO_2 SCR, was found to be quasi endothermic for two different reactions. It has to be noted in this context that the intermediates ST 20 and ST 21, which both include the interaction with NO_2, were obtained by descending the minimum energy pathway, starting from the transition states, of the corresponding subsequent reactions. Thus, it can be assumed in both cases that an additional transition to some adsorbed state of NO_2 exists, which is lower in energy than NH_2FeO (ST 19). For the subsequent reactions, however, this is assumed to not be of importance. With ST 20, an adsorbed state of NO_2 is illustrated, which exhibits one bond between its oxygen and the iron on the sextet PES. The subsequent reaction via TS 11 leads to the formation of an additional N−N bond between the adsorbed nitrogen dioxide and the amino group (ST 23). This step exhibits an energy barrier of $E^{\ddagger}$ = 3.7 kcal/mol (TS 11) but, with respect to the prior quasi endothermic adsorption of NO_2, has to be corrected to $E^{\ddagger}$ = 16.1 kcal/mol. This value can then be interpreted as the barrier of the reaction of NO_2 with NH_2FeO according to an Eley−Rideal type mechanism. The subsequent cleavage of the internal N−O bond of the adsorbed NO_2 results in nitrosamine adsorbed on OFeO (ST 26). The barrier for this step was calculated to be $E^{\ddagger}$ = 9.1 kcal/mol (TS 14). The remaining species OFeO easily recombines to FeO_2, and oxygen might desorb after a coadsorption of NO_2.[48] This corresponds to species ST 3 of part one (Figure 2), and the closure of the NO_2 reactive cycle without the production of nitrous oxide is contained in that part. Alternatively, the reaction of NO_2 with NH_2FeO might also lead to adsorbed nitramide on FeO (ST 24) which exhibits even a slightly lower barrier $E^{\ddagger}$ = 14.0 kcal/mol (TS 12) with respect to NH_2FeO. Furthermore, this step is exothermic in contrast to the endothermic pathway to nitrosamine. With that, not only is the initial formation of nitrosamine via TS 1 less likely than the formation of nitramide and the intermediate formation of water via TS 3 to TS 5 questionable with respect to high internal barriers, but also the second formation of nitrosamine via TS 11 and TS 14 is less likely than a competing formation of nitramide. From these results, it has to be concluded that the assumption of a pure NO_2 SCR mechanism that avoids the production of nitrous oxide, even at high temperatures, is questionable on mononuclear iron sites. This is also supported by the corresponding Gibbs' free energies at 600 K as shown in Figure 5, which are substantially higher in comparison to the values of part one (Figure 3). Thus, it remains indeed most plausible to assume the mechanism of the NO_2 SCR to proceed at low temperatures via the pathway as outlined in part one, including the production of equimolar amounts of nitrogen and nitrous oxide and at elevated temperatures the partial decomposition of NO_2 in accordance with Tronconi et al.[42] and Epling et al.,[37] which enables then the fast SCR mechanism. Furthermore, the decomposition of intermediately produced nitrous oxide could take place at high temperatures, and this will be briefly discussed in the fourth part.

Assuming that at high temperatures at least partially the initial step via TS 1 might take place, we also considered the interaction of NO with the resulting intermediate OFeOH (ST 3) on the quintet PES. This interaction eventually leads to the formation of a nitrite next to the hydroxyl group (ST 7), is strongly exothermic with ΔE = −30.8 kcal/mol, and only exhibits a very small barrier (TS 2, $E^{\ddagger}$ = 0.94 kcal/mol).[48] Thus, this species and the following pathways can also be seen in two further different contexts. First of all, HOFeONO on the sextet PES can be formed from the adsorption of NO_2 on monohydroxylated iron and marks an alternative pathway in the fast SCR as the one outlined in part one. Second, within the standard SCR, Delahay et al.[43] have stated the assumption that ammonia should react with some intermediate of the NO oxidation. This was intended to explain the observed significant deviations in activity of the catalyst for the NO oxidation and the standard SCR by an avoided desorption of NO_2 in the presence of NH_3. Brüggemann and Keil[48] have shown that also at 600 K the species HOFeONO exhibits the lowest Gibbs' free energy within the NO oxidation cycle on FeOH and could, thus, be the limiting nitrite species assumed by Delahay et al. Ammonia strongly coadsorbs to it (ST 10) with ΔE_{ads} = −17.8 kcal/mol. Subsequently, two different reactions, involving a hydrogen transfer, were considered. The first one involves the transfer from the ammonia to the hydroxyl group, forming water (TS 7) by overcoming a barrier of $E^{\ddagger}$ = 22.1 kcal/mol. The desorption of the produced water leads again to NH_2FeONO (ST 17), which is the precursor of a subsequent formation of nitrosamine. Alternatively, the proton transfer can take place to the adsorbed NO_2 by forming nitrous acid (ST 13). This step exhibits an activation energy of $E^{\ddagger}$ = 25.0 kcal/mol. The nitrous acid either then desorbs to the gas phase or further reacts from a transfer of its NO group to the amino group, which results in nitrosamine adsorbed on dihydroxylated iron (ST 18). This second step requires overcoming a barrier of $E^{\ddagger}$ = 9.1 kcal/mol. The desorption of NH_2NO eventually leads to the dihydroxylated iron in its ground state on the sextet PES. In both cases, the proton transfer exhibits a barrier, which is even slightly higher than the hydrogen transfer from ammonia, adsorbed on monohydroxylated iron as described in part one (Figure 2, TS 6). Within the fast SCR context, however, this would be the step potentially circumvented by first the adsorption of NO_2 prior to the proton transfer. It has to be concluded that this is from an energetic aspect not beneficial, but it reveals from a mechanistic view that NO_2 also does not block the further reaction. This implies that at lower temperatures the fast SCR indeed might partially proceed via TS7 or TS8. Within the NO oxidation, we have already shown that dihydroxylated iron can react with NO_x by forming nitrous or nitric acid. It also might react with ammonia after adsorption of the latter with the nitrogen bonded to the iron (ST 22) and a heat of adsorption of ΔE_{ads} = −15.2 kcal/mol. A hydrogen transfer from the ammonia to one of the hydroxyl groups results in the formation of water, adsorbed on NH_2FeOH (ST 25), and exhibits a barrier of $E^{\ddagger}$ = 21.2 kcal/mol. This barrier is about 2 kcal/mol lower in energy than the formation of NH_2FeOH from a hydrogen transfer of adsorbed ammonia on FeO, which was the initialization of the fast SCR mechanism of part one. In comparison, we[48] found for the

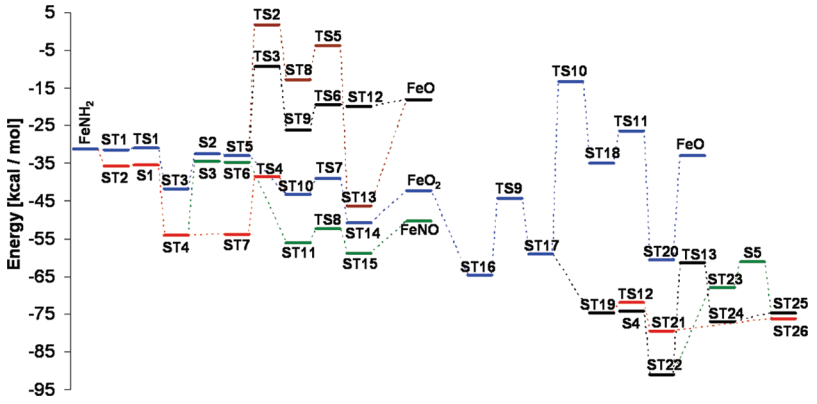

Figure 6. Energy profiles for the catalytic cycles of "part three: impact of oxygen". Energies are zero-point corrected.

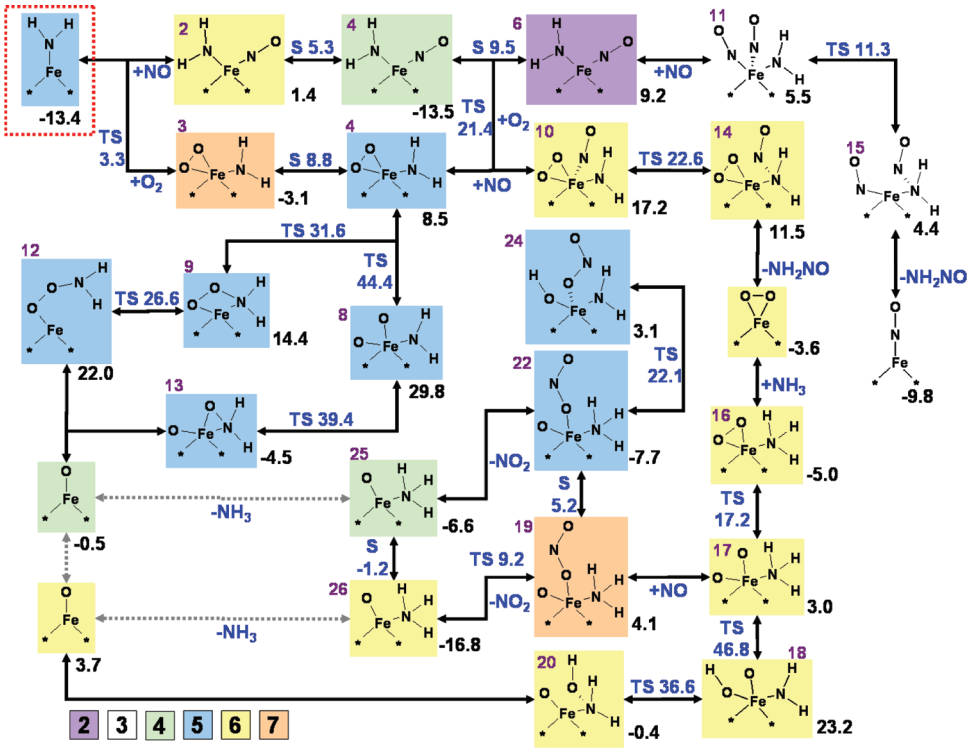

Figure 7. Overview of considered catalytic cycles of "part three: impact of oxygen". Stated values are Gibbs' free energies calculated at 600 K. Purple numbers refer to the structure labels of Figure 6. Black numbers correspond to the structure and blue numbers to the transition states (TS) or to the minimum on the seam of two PESs (S). Colors of the boxes correspond to the spin multiplicity.

formation of dihydroxylated iron from a reaction of FeO with water a rather low barrier of $E^{\ddagger}$ = 13.7 kcal/mol and concluded that this species potentially blocks the active site for the NO oxidation in the presence of water. Here, it can be seen that the occurrence of dihydroxylated iron is not expected to inhibit the SCR reaction because it is removed by ammonia.

Part 3: Impact of Oxygen. Oxygen was shown by Yang et al.[99] to be vital for the standard SCR to proceed on Fe/H-ZSM5, and it is believed that it serves the oxidation of NO to NO_2 as the rate-limiting step[38,43,46] of the overall reaction prior to accessing the mechanism of the fast SCR. Furthermore, oxygen also causes the oxidation of ammonia as an unwanted side reaction.[56] This section is intended to discuss on one hand the potential occurrence of a pathway for the standard SCR that is integrated into the described mechanism of the fast SCR rather than assuming a pure combination of the separated subreactions, NO oxidation and fast SCR. On the other hand, a potential initialization of the SCO of ammonia is outlined. The energies of all species are illustrated in Figure 6, and an overview of the reactions is shown in Figure 7. The corresponding structures of the species are shown in Figure S3 in the Supporting Information.

In part one, it was shown that the monohydroxylated iron marks, from an energetic point of view, a valley and that the reaction of ammonia with it leads to an amino group (Figure 2, $FeNH_2$) on the quintet PES. Within the presented catalytic cycle of the fast SCR this would be the adsorption site for the NO_2. This implies that, starting from FeO as an initial representation of

the active site, the pathway leading to $FeNH_2$ is identical for both cases, the fast and the standard SCR. Thus, in the absence of external NO_2, we consider $FeNH_2$ as the relevant initial species for a further pathway of the standard SCR. The adsorption of oxygen to this species is activated by a very low barrier of $E^{\ddagger} = 0.4$ kcal/mol (TS 1) and is slightly exothermic by $\Delta E = -10.3$ kcal/mol (ST 3). However, to further react with a nitrogen oxide, a spin change from the septet ground state to the quintet PES is required. The crossing of the seam between the two PESs exhibits a barrier of $E^{\ddagger} = 9.2$ kcal/mol (S 2) (electronic energy only), and the excited state (ST 5) is $\Delta E = 8.8$ kcal/mol higher in energy than the ground state. The adsorption of NO, bonded with the nitrogen to the iron (ST 10), is rather weak with respect to the ground state precursor. An alternative pathway up to this state was studied based on first the adsorption of NO to the $FeNH_2$. The ground state of the species NH_2FeNO was found to be on the quartet PES (ST 4), and thus, a spin change is required via S 1 and a negligible barrier of $E^{\ddagger} = 0.1$ kcal/mol. The adsorption of NO can be considered to be quite strong with a heat of adsorption to the ground state of $\Delta E_{ads} = -22.8$ kcal/mol. Oxygen does not interact with this species as can be seen from the energy profile of ST 7 in comparison to ST 4. Thus, the chemisorption of oxygen to the iron is an activated process illustrated with TS 4. This step exhibits an activation energy of $E^{\ddagger} = 15.5$ kcal/mol leading also to ST 10 in which both, oxygen and NO, are coadsorbed on the iron. This alternative pathway to ST 10 appears to be slightly more favorable because of the initial strong adsorption of NO. In a next step, the amino group and the adsorbed NO react by forming a N−N bond, which leads to nitrosamine, adsorbed on FeO_2 (ST 14). The barrier for this process is rather low with $E^{\ddagger} = 4.1$ kcal/mol and in analogy to the formation of nitrosamine on FeOH as outlined in part one. The desorption of nitrosamine leads to FeO_2 on the sextet PES.

Alternatively, starting from NH_2FeO_2 on the quintet PES (ST 5), we also considered the interaction of NO in terms of the formation of an −OONO ligand with the adsorbed oxygen in the trans configuration, followed by a conversion to the cis configuration and finally the desorption of NO_2 (not shown). These steps are in complete analogy to the mechanism of the NO oxidation on FeOH, and very similar barriers for the three steps on the two different adsorption sites were observed. However, in comparison to the formation of nitrosamine from NO with the amino group, no benefit could be deduced.

In the pathway leading eventually to FeO_2, to this point, the oxygen only served as an additional adsorbate, not interacting with the formation of nitrosamine. With respect to the strong adsorption of NO on $FeNH_2$, it is thus at hand to consider the direct formation of nitrosamine without the coadsorption of the oxygen. The heat of reaction, leading to a bare iron site together with gas phase nitrosamine, was calculated to be $\Delta E_R = 65.1$ kcal/mol. This value is too high to be reasonable for the reactive system, even at high temperatures and, thus, can be excluded. Alternatively, a second NO could adsorb on NH_2FeNO in its ground state. This, however, was found to require the prior transfer to the doublet PES (ST 6) via the MECP S 3 by overcoming an activation energy of $E^{\ddagger} = 10.4$ kcal/mol (electronic energy only). The subsequent adsorption of NO with the nitrogen bonded to the iron (ST 11) only exhibits a rather small heat of adsorption with respect to the precursor ground state (ST 11 vs ST 4). Then, nitrosamine forms from the amino group and one of the nitrogen oxides (ST 15) and desorbs, leaving FeNO in its ground state on the triplet PES. The barrier for this process was calculated to be $E^{\ddagger} = 3.8$ (TS 8) kcal/mol, which is again comparable to the formation of nitrosamine on FeOH or on FeO_2. However, due to the required spin change to the doublet PES prior to the adsorption of NO, this pathway is not severely beneficial over the above-described pathway. In fact, from the related energies, a higher probability has to be concluded for a redesorption of the first adsorbed NO over the coadsorption of a second one.

Assuming from the discussion above that FeO_2 on the sextet PES has formed after the reaction of the amino group with coadsorbed NO, the further formation of NO_2 from a reaction with NO was outlined in the context of the NO oxidation on FeO.[48] Alternatively, also ammonia can adsorb to this species (ST 16) with $\Delta E_{ads} = -22.3$ kcal/mol and its nitrogen bonded to the iron. For a subsequent hydrogen transfer, first, the cleavage of the two oxygen atoms in the adsorbed molecule is necessary (ST 17). This requires overcoming a barrier of $E^{\ddagger} = 20.3$ kcal/mol (TS 9), which is only slightly lower than the corresponding cleavage in the absence of ammonia ($\Delta E = 1.4$ kcal/mol), and thus, a beneficial influence of the ammonia cannot be observed. For the proton transfer from the adsorbed ammonia to one of the oxygen atoms (ST 18), we calculated a very high activation energy of $E^{\ddagger} = 45.9$ kcal/mol (TS 10) making this step very unlikely to proceed. Thus, the subsequent formation of hydroxylamine from the remaining amino group and the previously formed hydroxyl group (ST 20) via TS 11 and a barrier of $E^{\ddagger} = 8.6$ kcal/mol might rather be of interest in a different context than from the initial reaction of ammonia with FeO_2. Alternatively to the proton transfer, NO can coadsorb on one of the oxygen atoms, forming adsorbed NO_2 (ST 19). The ground state of this species is however located on the quintet PES (ST 22) rather than on the septet and is obtained from a spin change via S 4 ($E^{\ddagger} = 0.6$ kcal/mol, electronic energy only). The adsorption energy to the ground state was calculated to be $\Delta E_{ads} = -32.0$ kcal/mol. However, the desorption of NO_2 from this species results in an excited state of NH_3FeO on the quartet PES (ST 23), and another crossing of the seam to the sextet PES (ST 26) is required, which exhibits a barrier of $E^{\ddagger} = 6.7$ kcal/mol. Thus, overall, the desorption would require overcoming a barrier of $\Delta E_{des} = 30.0$ kcal/mol. NO_2 can however also desorb directly from the excited state of NH_3−OFeONO (ST 19), which is an activated process via TS 12 ($E^{\ddagger} = 2.8$ kcal/mol). With respect to the ground state, the NO_2 desorption requires overcoming $\Delta E_{des} = 19.2$ kcal/mol, making the latter pathway more favorable. Finally, we also considered the proton transfer from the ammonia to the oxygen atom on the iron on ST 19 and found the barrier via TS 13 with $E^{\ddagger} = 35.2$ kcal/mol to be substantially less favorable than the desorption of NO_2. Thus, with respect to the interaction of ammonia with FeO_2 the most favorable pathway resulted eventually solely in the oxidation of NO to NO_2, and it has to be concluded that this rather proceeds in the absence of ammonia directly on FeO_2 via the −OONO ligand as outlined in our previous paper.[48]

In summary, the described formation of nitrosamine from adsorbed NO and the initially considered amino group, eventually leading to FeO_2, could be significant in the standard SCR. Integrated into the mechanism of the fast SCR, it allows for the access to the NO oxidation in the absence of water for one further molecule of nitric oxide, which is known to be significantly faster than the NO oxidation in the presence of water.[39,41,45,47,48] This, however, also depends on the fraction of available $FeNH_2$ on the catalyst, which can only be answered from a microkinetic model.

Furthermore, a major drawback in the considered formation of the intermediate FeO_2 together with nitrosamine remains the necessary initial coadsorption of NO and O_2 on $FeNH_2$. With respect to entropy, this is a rather unfavorable process at elevated temperatures, considering that the combined heat of adsorption of the two molecules is rather low (ST10 vs $FeNH_2$). In contrast, an interaction of ammonia with FeO_2 can be excluded within the standard SCR. This is also supported by the rather high Gibbs' free energies as shown in Figure 7.

A reaction of the amino group with only NO resulted in a bare iron ion and was concluded to be very unlikely with respect to its endothermic character. The interaction of the amino group with adsorbed oxygen can, however, potentially be seen as the initialization of the ammonia oxidation. Two different pathways were analyzed in this context. In the first one, the cleavage of the oxygen molecule into two oxygen atoms on the iron (ST 8) was considered, starting from ST5. This process exhibits an activation energy of $E^{\ddagger}$ = 34.6 kcal/mol (TS 2) and is endothermic by ΔE = 20.1 kcal/mol. A subsequent formation of a bond between one of the oxygen atoms and the amino group leads to the adsorbed radical H_2NO (ST 13) by overcoming a barrier of $E^{\ddagger}$ = 8.9 kcal/mol (TS 5). The rather high desorption energy with ΔE_{des} = 28.0 kcal/mol of the radical, resulting in FeO on the quartet PES, indicates the high stability of the adsorbed state. Alternatively, we found a mechanism for the formation of the H_2NO radical from first the formation of a bond between the amino group with the oxygen molecule. Here, the barrier is significantly lower with $E^{\ddagger}$ = 23.4 kcal/mol (TS 3), leading to a state in which an $-OONH_2$ ligand is 2-fold bonded to the iron with the nitrogen and one oxygen (ST 9). Breaking the iron−nitrogen bond exhibits a barrier of $E^{\ddagger}$ = 6.7 kcal/mol (TS 6), and the final desorption of H_2NO also leads to FeO on the quartet PES. The produced radical was already shown on the H-form catalyst to be a significant intermediate in the NH_3 oxidation,[78] and its further decomposition will be discussed in the fourth part. It can be concluded that the formation of this radical is significantly more favorable from the reaction via the $-$-$OONH_2$ in analogy to the mechanism of the NO oxidation.[48] Although the energy profiles in Figure 6 as well as the Gibbs' free energies at 600 K shown in Figure 7 indicate that the formation of H_2NO is not favorable over the pathway to FeO_2 within the SCO, these steps might be significant and at temperatures above 600 K also become dominating because of the impact of entropy.

Part 4: Aspects of SCO and N_2O Decomposition. In part three, we have shown with respect to the influence of oxygen that the radical H_2NO can be formed from a reaction of the intermediate $FeNH_2$ of the fast SCR with O_2. Because this radical also occurs within the SCO of ammonia on the Brønsted acids,[78] we assumed its formation on the mononuclear iron site to mark the potential initialization of the SCO on iron. In this part, we focus on the fate of H_2NO and outline potential pathways that account for the SCO of ammonia and involve, in analogy to the results on the Brønsted acids, also the formation of the intermediate nitroxyl. Furthermore, in part one, the formation of nitrous oxide in the NO_2 SCR from the formation and decomposition of nitramide was discussed. As it is known that N_2O decomposes on Fe-ZSM5,[61−63,93,96] but is also reduced in a SCR with ammonia,[64−67] we also outline here some aspects of the fate of nitrous oxide. This should, however, rather be seen in the context of the NO_x SCR than as standing for itself. An overlap to the SCO is evident in view of the explanations of Coq et al.[64] for the mechanism of the N_2O SCR, which involves the oxidation of ammonia from the released oxygen of nitrous oxide.

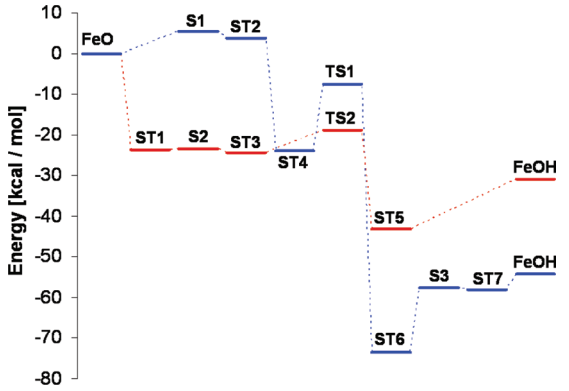

Figure 8. Energy profiles for the decay of H_2NO and HNO on $Z^-[FeO]^+$. Energies are zero-point corrected.

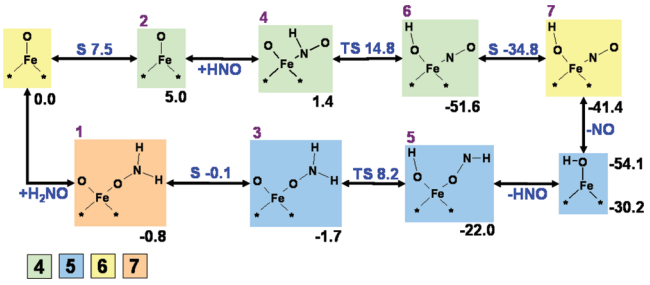

Figure 9. Overview of the decay of H_2NO and HNO on $Z^-[FeO]^+$. Stated values are Gibbs' free energies calculated at 600 K. Purple numbers refer to the structure labels of Figure 8. Black numbers correspond to the structure and blue numbers to the transition states (TS) or to the minimum on the seam of two PESs (S). Colors of the boxes correspond to the spin multiplicity.

For the potential decay of the radical H_2NO and the subsequently produced nitroxyl, we considered the interaction with first FeO and then with FeOH. For the interaction with FeO, the energies are shown in Figure 8 and the overview in Figure 9. The structures of the species are shown in Figure S4 in the Supporting Information. The adsorption of H_2NO on FeO (M_S = 6) in its ground state with the oxygen bonded to the iron exhibits a quite high heat of adsorption of ΔE_{ads} = −23.8 kcal/mol (ST 1). However, on the septet PES this species $OFeONH_2$ does not represent the ground state, and the crossing to the quintet PES is required. The barrier for this step was found to be negligible with $E^{\ddagger}$ = 0.3 kcal/mol (electronic energy only), and the final ground state on the quintet PES (ST 3) is only ΔE = 0.7 kcal/mol lower in energy than on the septet PES. In fact, based on DFT, such a small difference is not sufficient to conclude the true ground state, but this is not of significant relevance within the qualitative discussion on the reaction mechanism. Subsequently, a proton transfer from the H_2NO to the oxygen of FeO takes place, which involves an energy barrier of $E^{\ddagger}$ = 5.6 kcal/mol (TS 2) and is exothermic by ΔE = −18.8 kcal/mol. This leads, in consequence, to nitroxyl being adsorbed on monohydroxylated iron (ST 5) with its oxygen bonded to the iron. The final desorption of nitroxyl requires overcoming the heat of desorption ΔE_{des} = 12.2 kcal/mol. Besides its interaction with $FeNH_2$ as shown in part one, the produced nitroxyl can also interact with FeO. However,

for the adsorbed nitroxyl as well as for the subsequent reaction, we found the ground state to be on the quartet PES. Previously, we have shown that FeO on the quartet PES is only slightly higher in energy than the ground state[48] (ΔE = 3.8 kcal/mol, ST 2), and the barrier for the crossing is rather low as well ($E^{\ddagger}$ = 5.4 kcal/mol, S1). Nitroxyl adsorbs then rather strongly to FeO with ΔE_{ads} = −23.9 (ST 4) with respect to the ground state of the initial active site. In fact, similar as for H_2NO, it can be assumed that nitroxyl also directly adsorbs to FeO on the sextet PES and that a subsequent MECP can transfer the reactant OFeHNO to the required quartet PES, but this is believed to be of minor significance in this context. Similarly, also H_2NO could have been considered to directly adsorb to the quartet FeO, leading to ST 3. Nevertheless, the hydrogen transfer from the adsorbed nitroxyl in OFeHNO to the free oxygen leads to the ground state of NO, adsorbed on monohydroxylated iron (ST 6). This step is strongly exothermic by ΔE = −49.5 kcal/mol after overcoming a barrier of $E^{\ddagger}$ = 16.5 kcal/mol (TS 1). For the desorption of nitric oxide, however, another spin change to the sextet PES is required because monohydroxylated iron is in its ground state on the quintet PES. This barrier via S 3 was calculated to be $E^{\ddagger}$ = 15.8 kcal/mol, and NO then subsequently desorbs. With that, it was shown that intermediately produced H_2NO easily decomposes on FeO to monohydroxylated iron and nitroxyl. The latter potentially reacts with another FeO to nitric oxide and FeOH. Also the Gibbs' free energies, as shown in Figure 9, reveal that both pathways exhibit rather low barriers and are strictly exothermic, making them very likely to occur. Produced NO can be consumed further within the mechanism of the standard SCR. The main bottleneck in the context of the SCO, however, has to be seen in the low probability of FeO being present as a free site for the adsorption because the high concentrations of the reactant ammonia make it certainly more likely to be blocked by the latter.

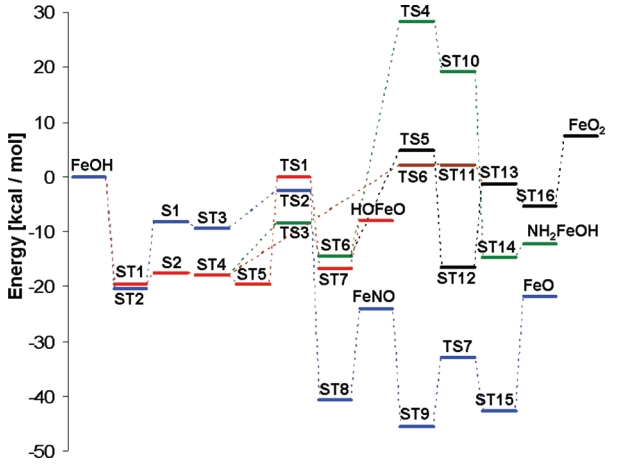

Figure 10. Energy profiles for the decay of H_2NO and HNO on $Z^{-}[FeOH]^{+}$. Energies are zero-point corrected.

Furthermore, we have analyzed the interaction of the two intermediates H_2NO and HNO with monohydroxylated iron. The corresponding energies are displayed in Figure 10, and the schematic overview is shown in Figure 11. The structures of the species are shown in Figure S5 in the Supporting Information. In contrast to all prior discussed pathways, the energies in both figures are here calculated with respect to FeOH as the active site rather than FeO. The radical H_2NO adsorbs to the FeOH with its oxygen bonded to the iron and a heat of adsorption of ΔE_{ads} = −19.5 kcal/mol (ST 1) representing the ground state of the adsorbed species on the sextet PES. For a subsequent reaction, it was found necessary to consider a spin change to the quartet PES which is, however, only slightly higher in energy (ST 4). Also, the barrier for the crossing was found to be rather low with $E^{\ddagger}$ = 1.9 kcal/mol (S 2). Then, a reaction with nitric oxide forms nitrosamine together with HOFeO. From the energy profile, it can be concluded that NO hardly interacts with the surface species (ST 5), and thus, the reaction can be interpreted to be of the Eley−Rideal type. For the barrier of the cleavage of the O−N bond in the adsorbed radical H_2NO together with the simultaneous formation of a N−N bond with the gas phase nitric oxide, a value of $E^{\ddagger}$ = 19.3 kcal/mol (TS 1) was obtained. After the

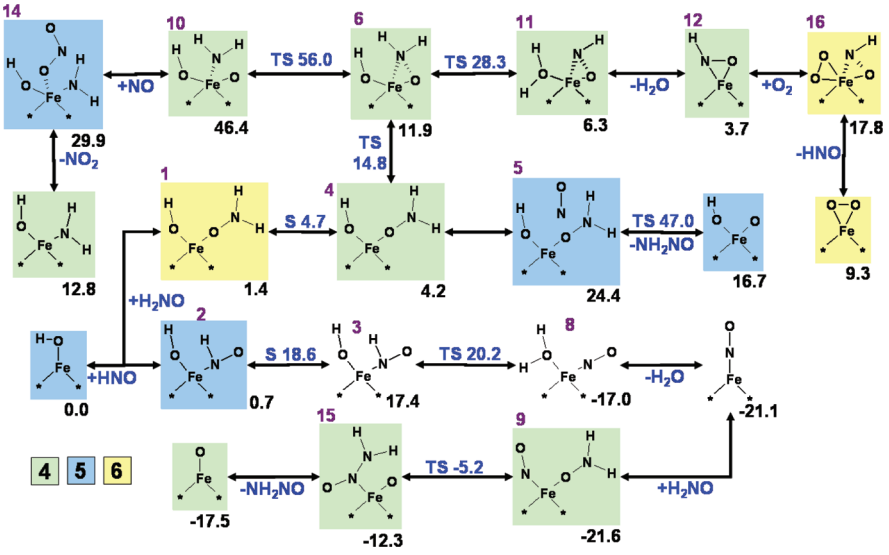

Figure 11. Overview of the decay of H_2NO and HNO on $Z^{-}[FeOH]^{+}$. Stated values are Gibbs' free energies calculated at 600 K. Purple numbers refer to the structure labels of Figure 10. Black numbers correspond to the structure and blue numbers to the transition states (TS) or to the minimum on the seam of two PESs (S). Colors of the boxes correspond to the spin multiplicity.

dx.doi.org/10.1021/jp206931z |J. Phys. Chem. C 2011, 115, 23854–23870

desorption of nitrosamine, the remaining HOFeO could react with another NO to form NO_2 together with monohydroxylated iron. However, the high Gibbs' free energy at 600 K for the transition state suggests that this formation of nitrosamine is rather unlikely. The reason can be seen in the required coadsorption of two molecules prior to the reaction causing a high loss in entropy in the transition state as compared to the reactant state. Alternatively, we considered the decomposition of the adsorbed H_2NO. In a first step, starting from ST 4, the radical forms a second bond to the iron with its nitrogen (ST 6). The barrier for this process is $E^{\ddagger}$ = 11.1 kcal/mol (TS 3), and the product is only slightly higher in energy by ΔE = 4.9 kcal/mol. The cleavage of the internal O−N bond (ST 10) in contrast was found to be highly endothermic by ΔE = 33.8 kcal/mol, dictating in addition a quite high energy barrier for this step with $E^{\ddagger}$ = 42.7 kcal/mol (TS 4). Although a subsequent adsorption of NO on the free atomic oxygen (ST 14) and the subsequent desorption of NO_2 from the remaining NH_2FeOH is strongly exothermic, the intermediate formation of the HOFeO−NH_2 (ST 10) is rather unlikely and can be excluded. This is also expressed in the high Gibbs' free energies for this pathway as shown in Figure 11. Finally, the proton transfer from the adsorbed H_2NO to the hydroxyl group on the iron remains, leading to coadsorbed water and nitroxyl. For this process, two different pathways were analyzed on the quartet PES. The first one starts from ST 4, in which the radical is only bonded to the iron with its oxygen. The proton transfer exhibits a barrier of $E^{\ddagger}$ = 20.2 kcal/mol (TS 6, electronic energy only), and the resulting product has to be considered rather unstable because of a negligible reverse barrier. In fact the desorption of water from this product state (ST 11) was found to be endothermic (ST 11 vs ST 13), which suggests a further reaction step prior to the water desorption. Alternatively, the proton transfer and the desorption of water to the gas phase can be interpreted as a combined step. The second pathway starts with a proton transfer from the 2-fold bonded radical (ST 6) which includes a barrier of $E^{\ddagger}$ = 19.5 kcal/mol (TS 5). The resulting product state (ST 12) requires a heat of desorption for the water of ΔE_{des} = 15.1 kcal/mol (ST 13). The remaining nitroxyl on the iron can be exchanged with oxygen by coadsorption of the latter (ST 16) and desorption of HNO to FeO_2 which is part of the NO oxidation pathway. Overall, both pathways for the proton transfer are energetically similar and can be accessed. Also, with respect to the Gibbs' free energies at 600 K, it has to be concluded that the most probable decay of H_2NO on monohydroxylated iron results from the proton transfer to the hydroxyl group eventually forming nitroxyl. In comparison to the analogue proton transfer on FeO, however, the barrier is significantly higher, and thus the impact of this pathway remains anchored to the surface concentrations of FeO and FeOH.

A slightly different behavior was found for the interaction of nitroxyl with the monohydroxylated iron. It also adsorbs quite strongly to the active site (ΔE_{ads} = −20.3 kcal/mol, ST 2) with its nitrogen bonded to the iron. Then, a spin change from the quintet to the triplet PES is required prior to the subsequent reaction because the final product has its ground state on the lower PES. The crossing of the seam exhibits a barrier of $E^{\ddagger}$ = 12.1 kcal/mol (S 1, electronic energy only), and the excited state (ST 3) is ΔE = 10.9 kcal/mol higher in energy than the ground state. In the subsequent reaction, a proton transfer from the nitroxyl to the hydroxyl group takes place, which leads to water adsorbed on FeNO (ST 8) on the triplet PES. For this transfer, a barrier of $E^{\ddagger}$ = 7.0 kcal/mol needs to be overcome, and a reverse

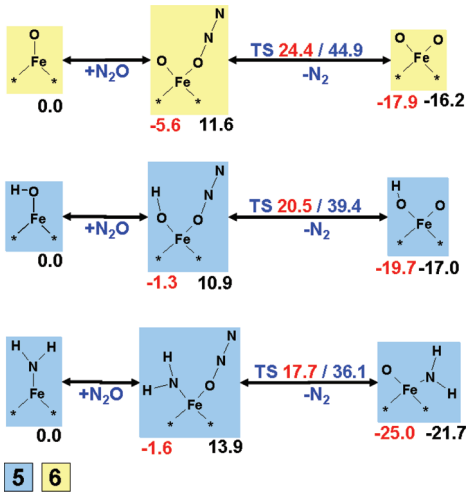

Figure 12. Overview of the decay of N_2O on $Z^-[FeO]^+$, $Z^-[FeOH]^+$, and $Z^-[FeNH_2]^+$. Stated values are zero-point corrected energies (red) and Gibbs' free energies calculated at 600 K. Black numbers correspond to the structure and blue numbers to the transition states (TS) or to the minimum on the seam of two PESs (S). Colors of the boxes correspond to the spin multiplicity.

reaction is rather unlikely because of its strong exothermicity (ΔE = −31.2 kcal/mol). Finally, water desorbs, leaving FeNO as the surface species. In fact, this pathway is in close analogy to the reaction of nitroxyl with $FeNH_2$, as described in part one, with respect to both the mechanism and the corresponding barriers. Furthermore, the combined barrier of spin inversion (S 1) and proton transfer is with $E^{\ddagger}$ = 17.9 kcal/mol quite similar to the barrier of the proton transfer on FeO. Thus, for the decay of nitroxyl the impact of available surface concentrations, as was outlined for H_2NO, is less significant. The produced FeNO can be transferred back to FeO within the mechanism of the NO oxidation.[48] Alternatively, a reaction with the radical H_2NO can take place after its strong adsorption (ΔE_{ads} = −21.5 kcal/mol) with the oxygen bonded to the iron (ST 9). The formation of a N−N bond between the amino group of the adsorbed radical and the NO leads to the formation of nitrosamine, which remains bonded with a nitrogen to the iron (ST 15). This step exhibits a barrier of $E^{\ddagger}$ = 12.5 kcal/mol (TS 7), and the final desorption of nitrosamine (ΔE_{des} = 20.9 kcal/mol) restores FeO in the quartet state. This final process certainly might be of significant impact for both the further decay of the radical H_2NO and the intermediately produced surface species FeNO, as can be also concluded from the low Gibbs' free energies in Figure 11. However, the high oxygen concentrations in the reactant feed gas of the SCO make the consumption of FeNO from O_2 more probable. Nevertheless, starting from the production of the radical H_2NO as described in part three, the consumption of ammonia to first nitroxyl and then to NO can be concluded to be a reasonable explanation of the mechanism of the SCO in accordance to the suggestions of Akah et al.[57] and Yang et al.[59] A closure of the reactive cycle is obtained with respect to the production of $FeNH_2$, as the precursor to the H_2NO formation, as outlined in part one. Produced NO is consumed in the pathway starting from FeO via FeOH to finally $FeNH_2$.

For the decay of nitrous oxide, as is produced in the NO_2 SCR, the release of its oxygen to the catalytic surface is the most reasonable concept as was shown by Heyden et al.[61,62]

In Figure 12, the schematics with the corresponding zero-point corrected energies (red) and the Gibbs' free energies at 600 K are shown for this step on the initial sites FeO, FeOH, and $FeNH_2$. While the barrier for the oxygen release is severely higher on FeO with $E^{\ddagger}$ = 31.1 kcal/mol, they are rather similar for the two other species (FeOH: $E^{\ddagger}$ = 21.8 kcal/mol; $FeNH_2$: $E^{\ddagger}$ = 19.3 kcal/mol). Thus, for the latter two species, the barriers are within the order of magnitude of the two highest internal barriers within the presented fast and NO_2 SCR mechanism in part one and, with that, can be concluded to be accessible. With respect to the fact that in part one monohydroxylated iron was concluded to probably be the most abundant intermediate, at elevated temperatures, the decay of nitrous oxide on this species to a certain extent is likely. Heyden et al.[62] have shown for the NO assisted N_2O decomposition on mononuclear iron sites that a crucial step is the decomposition of NO_2 on HOFeO via an −OONO ligand. The initial surface species was the product of the oxygen release of N_2O on FeOH. In fact, we also found this step via the −OONO ligand to mark a crucial point in the NO oxidation on FeOH,[48] although in the reverse direction. However, it can be derived from this analysis that in the NO_2 SCR the decreasing selectivity to nitrous oxide with increasing temperature can be related to two different reactions. The thermodynamic equilibrium dictates the decomposition of NO_2 to NO and oxygen to a certain extent. On the other hand, formed nitrous oxide might decompose on monohydroxylated iron, forming HOFeO together with nitrogen. This latter produced surface species, however, is also the adsorption site for a second NO_2 molecule within the decomposition cycle of nitrogen dioxide on FeOH. With that, a mixture of NO_2 and N_2O decomposition, with the latter making use of the significantly higher activity of the NO-assisted pathway, can be deduced to explain the decrease in observed nitrous oxide in the NO_2 SCR with increasing temperature.

In summary, we have studied several pathways on the basis of the DFT within the SCR of NO_x with ammonia on Fe-ZSM5. Iron was represented as mononuclear iron sites, and it was assumed that NH_2NO_x are essential intermediates that decompose on the Brønsted acids as shown in our previous investigations.[24,25] In part one, a low energy pathway was presented in accordance with the stoichiometry of the fast SCR. In analogy, a pathway for the NO_2 SCR, leading to equimolar amounts of nitrogen and nitrous oxide, can be concluded to be equivalent to the fast SCR in its main steps but to differ in the formation of one nitramide from a reaction of a surface amino group with NO_2 rather than the formation of nitrosamine from NO. For the fast SCR, Li and Li[76] have proposed a pathway that also leads to the intermediate formation of nitrosamine and involves mononuclear FeO and FeOH. However, as essential steps, they assumed the coadsorption of NO and ammonia on FeO and FeOH prior to a direct formation of nitrosamine. The initial adsorbed state of NO on FeO, as presented in their work, was concluded in a preceding study on the NO oxidation[48] to be highly unstable because only a low barrier of $E^{\ddagger}$ = 3.9 kcal/mol needs to be overcome to form the significantly more stable nitrite. Thus, the initial state of the mechanism has to be considered rather unlikely to be available for the subsequent coadsorption of ammonia. Furthermore, with respect to the loss of entropy from adsorption, the assumption of the coadsorption of two molecules prior to a reaction, as done by Li and Li, is less likely than the here outlined mechanism which always considers, first, the formation of an amino group on the iron prior to a subsequent interaction with NO_x.

For the change of selectivity in the NO_2 SCR toward molecular nitrogen with increasing temperature, it was found in part two that an additional reaction mechanism, leading directly to N_2, is unlikely to proceed. This behavior can rather be explained by a combined decomposition of intermediately produced N_2O and of the reactant NO_2 into NO and oxygen as outlined in part four.

In part three, a potential reaction mechanism for the standard SCR, integrated into the steps of the fast SCR, was addressed. Nitrosamine might be formed after the coadsorption of NO and oxygen on $FeNH_2$. This can be interpreted to be in accordance with Schwidder et al.,[8] who concluded from the observed strong deviation between NO oxidation and standard SCR activity that the latter might not solely be a combination of NO oxidation followed by the fast SCR. Although our proposed mechanism would circumvent this crude combination of subreactions in series, some doubt is left with respect to an unfavorable impact of entropy for the required coadsorption of NO and O_2. A final conclusion on this question can only be drawn from microkinetic modeling of the system which is the ambition of our current research.

In addition, we have also shown that from a reaction of oxygen with the $FeNH_2$ the intermediate radical H_2NO can be formed, which further decomposes to nitroxyl and eventually is reduced to NO as outlined in part four. Thus, the formation of the H_2NO can be seen as the potential initialization of the SCO with the intermediately formed NO being consumed within the standard SCR. This is in agreement to the conclusions of Akah et al.[56,57] and Yang et al.[59] who proposed, first, the oxidation of ammonia to nitric oxide and its subsequent consumption by ammonia to molecular nitrogen within the standard SCR.

The proposed mechanisms for the SCR schemes in the literature are all quite similar.[7,40,42,71] It is assumed that ammonium nitrate and nitrite or surface nitrates and nitrites are formed, which are created from the disproportionation of two NO_2. The reduction of the nitrates by NO is believed to be the rate-determining step in the fast SCR. We have outlined that such a step exhibits a significantly higher barrier[48] than the highest internal barrier in our proposed mechanism. Thus, it was concluded that the significant role of the nitrate reduction as stressed by Tronconi et al.[71] is rather unlikely. Also, the concept of the disproportionation of two NO_x and the formation and decomposition of ammonium nitrite and nitrate fit to our results for the fast and NO_2 SCR on the Brønsted acids[24,25,79] rather than to the outlined pathway on the iron sites. However, it has to be emphasized that our presented mechanism only refers to the analysis of mononuclear iron sites, while on dinuclear iron or iron clusters the mechanism could be completely different.

Furthermore, Tronconi et al.[53,54] have presented a new "enhanced" SCR in which, besides ammonia, also ammonium nitrate is applied as reducing agent, and they observed a significantly higher conversion as for the standard SCR. An explanation of this mechanism can also be derived from our mechanism as outlined in part one within the assumption that evaporated ammonium nitrate decomposes into ammonia and nitric acid. Following the sequence of steps in Figure 3, it is at hand that from two ammonia molecules and one NO the species $FeNH_2$ is easily produced together with water and nitrosamine. Then, nitric acid adsorbs to this species and releases NO_2 to the gas phase, which restores the species NH_2FeOH for the reaction

with another NO. Eventually, again the species $FeNH_2$ is produced, which now reacts with the previously released NO_2. After the desorption of the produced nitrosamine to the gas phase, the catalytic cycle is closed. Thus, the schematic directly also explains the new "enhanced" SCR within the observed stoichiometry (eq 4). Alternatively, the nitric acid could also adsorb on monohydroxylated iron forming a dihydroxylated iron after the release of NO_2. In part two, it was shown that ammonia reacts with the dihydroxylated iron by forming water and again the intermediate NH_2FeOH.

CONCLUSION

The reaction mechanism of the selective catalytic reduction of nitrogen oxide on iron-exchanged ZSM5 was investigated using the density functional theory. All reaction steps were studied on a cluster of five T-atoms, containing a mononuclear iron ion. The crossing of PESs was considered, if necessary. While the NO oxidation, which is considered as the rate-determining step of the standard SCR,[38,39,43−45] was already discussed in a previous paper,[48] we have presented here a mechanism for the fast and NO_2 SCR starting from $Z^-[FeO]^+$ as a representation of the active site on the sextet PES. It was concluded that most probably, first, ammonia adsorbs to the active site, and a proton transfer takes place to the oxygen forming an amino group next to a hydroxyl group. Then, either NO or NO_2 reacts with this intermediate forming nitrosamine or nitramide, respectively, and monohydroxylated iron remains. The reaction with another ammonia results in the formation of water, and an amino group remains on the iron. The latter finally reacts with NO_2 to nitrosamine, and the active site is restored. Nitrosamine and nitramide are assumed to decompose on Brønsted acids into nitrogen and nitrous oxide, respectively, together with water. To account for the increasing selectivity of the NO_2 SCR to nitrogen over nitrous oxide with temperature, we concluded that not an additional reaction mechanism, leading directly to only nitrogen, is responsible for this behavior. It is rather the result of an interacting combination of nitrous oxide decomposition and NO_2 decomposition from thermodynamic limitations,[37,42] on monohydroxylated iron. In this context, the analogy to the NO-assisted nitrous oxide decomposition was outlined.[62] Furthermore, it could be shown that the additional consideration of the decomposition of nitric acid on either the $Z^-[FeNH_2]^+$ or on monohydroxylated iron also allows for the explanation of the mechanism of the recently proposed new "enhanced" SCR.[53] For the impact of oxygen, starting from the intermediate surface species $Z^-[FeNH_2]^+$, the formation of the radical H_2NO was proposed to mark the initialization of the selective catalytic oxidation of ammonia on the catalyst. The radical was shown to further decompose to nitroxyl and eventually lead to NO. Nitric oxide might then further be consumed within the mechanism of the SCR in accordance with the experimental literature.[57,59] Finally, we have also discussed an alternative pathway for the standard SCR, integrated into the scheme of the fast SCR rather than requiring the NO oxidation separately. Starting from the intermediate $Z^-[FeNH_2]^+$, after the coadsorption of NO and O_2 the reaction of the amino group with nitric oxide forms nitrosamine. The remaining adsorbed oxygen reacts with NO to NO_2, which is released and restores the initial active site. Thus, only half of the separate NO oxidation is required but takes place via the mechanism of the water-free NO oxidation, which is significantly faster than on the monohydroxylated iron. The impact of such an additional pathway can however only be revealed from microkinetic modeling. With that, we have presented a theoretical investigation of the SCR of NO with ammonia on mononuclear iron sites, exchanged into ZSM5, which accounts for many experimentally observed phenomena.

ASSOCIATED CONTENT

Supporting Information. Figures of the structure of all the intermediates, transition states, and minimum energy crossing points. This material is available free of charge via the Internet at http://pubs.acs.org.

AUTHOR INFORMATION

Corresponding Author
*E-mail: till.brueggemann@tu-harburg.de

ACKNOWLEDGMENT

The computations were partly carried out at the Norddeutscher Verbund für Hoch- und Höchstleistungsrechnen (HLRN). We thank Marc-Andreas Christlieb for the contribution of some calculations.

REFERENCES

(1) Busca, G.; Lietti, L.; Ramis, G.; Berti, F. *Appl. Catal., B* **1998**, *18*, 1–36.
(2) Hu, Y.; Griffiths, K.; Norton, P. R. *Surf. Sci.* **2009**, *603*, 1740–1750.
(3) Schwefer, M.; Siefert, R.; Groves, M.; Maurer, R. *Chem. Ing. Tech.* **2004**, *76*, 1283.
(4) Liu, Z. M.; Woo, S. I. *Catal. Rev. Sci. Eng.* **2006**, *48*, 43–89.
(5) Kröcher, O.; Elsener, M. *Ind. Eng. Chem. Res.* **2008**, *47*, 8588–8593.
(6) Iwasaki, M.; Yamazaki, K.; Shinjoh, H. *Appl. Catal., B* **2011**, *102*, 302–309.
(7) Brandenberger, S.; Kröcher, O.; Tissler, A.; Althoff, R. *Catal. Rev. Sci. Eng.* **2008**, *50*, 492–531.
(8) Schwidder, M.; Heikens, S.; Toni, A. d.; Geisler, S.; Berndt, M.; Brueckner, A.; Gruenert, W. *J. Catal.* **2008**, *259*, 96–103.
(9) Grossale, A.; Nova, I.; Tronconi, E.; Chatterjee, D.; Weibel, M. *Top. Catal.* **2009**, *52*, 1837–1841.
(10) Kustov, A. L.; Egeblad, K.; Kustova, M.; Hansen, T. W.; Christensen, C. H. *Top. Catal.* **2007**, *45*, 159–163.
(11) Lima, E.; Guzmán-Vargas, A.; Méndez-Vivar, J.; Pfeiffer, H.; Fraissard, J. *Catal. Lett.* **2008**, *120*, 244–251.
(12) Brandenberger, S.; Kröcher, O.; Tissler, A.; Althoff, R. *Ind. Eng. Chem. Res.* **2011**, *50*, 4308–4319.
(13) Kumar, M. S.; Schwidder, M.; Grünert, W.; Brückner, A. *J. Catal.* **2004**, *227*, 384–397.
(14) Capek, L.; Kreibeich, V.; Dedecek, J.; Grygar, T.; Wichterlova, B.; Sobalik, Z.; Martens, J.; Brosius, R.; Tokarova, V. *Microporous Mesoporous Mater.* **2005**, *80*, 279–289.
(15) Iwasaki, M.; Yamazaki, K.; Banno, K.; Shinjoh, H. *J. Catal.* **2008**, *260*, 205–216.
(16) Krishna, K.; Makkee, M. *Catal. Today* **2006**, *114*, 23–30.
(17) Iwasaki, M.; Shinjoh, H. *J. Catal.* **2010**, *273*, 29–38.
(18) Toni, A. d.; Schwidder, M.; Grünert, W.; Brückner, A. *Chem. Ing. Tech.* **2007**, *79*, 871–877.
(19) Lobree, L. J.; Hwang, I. C.; Reimer, J. A.; Bell, A. T. *J. Catal.* **1999**, *186*, 242–253.
(20) Brandenberger, S.; Kröcher, O.; Tissler, A.; Althoff, R. *Appl. Catal., B* **2010**, *95*, 348–357.

(21) Brandenberger, S.; Kröcher, O.; Tissler, A.; Althoff, R. *Appl. Catal., A* **2010**, *373*, 168–175.
(22) Schwidder, M.; Kumar, M. S.; Klementiev, K.; Pohl, M.; Brückner, A.; Grünert, W. *J. Catal.* **2005**, *231*, 314–330.
(23) Kumar, M. S.; Schwidder, M.; Grünert, W.; Bentrup, U.; Brückner, A. *J. Catal.* **2006**, *239*, 173–186.
(24) Brüggemann, T. C.; Keil, F. J. *J. Phys. Chem. C* **2008**, *112*, 17378–17387.
(25) Brüggemann, T. C.; Przybylski, M.-D.; Balaji, S. P.; Keil, F. J. *J. Phys. Chem. C* **2010**, *114*, 6567–6587.
(26) Stevenson, S.; Vartuli, J. C. *J. Catal.* **2000**, *190*, 228–239.
(27) Stevenson, S.; Vartuli, J. C. *J. Catal.* **2002**, *208*, 100–105.
(28) Eng, J.; Bartholomew, C. H. *J. Catal.* **1997**, *171*, 14–26.
(29) Eng, J.; Bartholomew, C. H. *J. Catal.* **1997**, *171*, 27–44.
(30) Wallin, M.; Karlsson, C.; Skoglundh, M.; Palmqvista, A. *J. Catal.* **2003**, *218*, 354–364.
(31) Wallin, M.; Karlsson, C.-J.; Palmqvist, A.; Skoglundh, M. *Top. Catal.* **2004**, *30/31*, 107–113.
(32) Sullivan, J.; Keane, O. *Appl. Catal., B* **2005**, *61*, 244–252.
(33) Brandenberger, S.; Kröcher, O.; Wokaun, A.; Tissler, A.; Althoff, R. *J. Catal.* **2009**, *268*, 297–306.
(34) Schwidder, M.; Kumar, M. S.; Bentrup, U.; Pérez-Ramírez, J.; Brückner, A.; Grünert, W. *Microporous Mesoporous Mater.* **2008**, *111* 124–133.
(35) Long, R.; Yang, R. T. *J. Catal.* **2002**, *207*, 224–231.
(36) Schuler, A.; Votsmeier, M.; Kiwic, P.; Gieshoff, J.; Hautpmann, W.; Drochner, A.; Vogel, H. *Chem. Eng. J.* **2009**, *154*, 333–340.
(37) Luo, J.-Y.; Hou, X.; Wijayakoon, P.; Schmieg, S. J.; Li, W.; Epling, W. S. *Appl. Catal., B* **2011**, *102*, 110–119.
(38) Rahkamaa-Tolonen, K.; Maunula, T.; Lomma, M.; Huuhtanen, M.; Keiski, R. *Catal. Today* **2005**, *100*, 217–222.
(39) Devadas, M.; Kröcher, O.; Elsener, M.; Wokaun, A.; Soger, N.; Pfeifer, M.; Demel, Y.; Mussmann, L. *Appl. Catal., B* **2006**, *67*, 187–196.
(40) Iwasaki, M.; Shinjoh, H. *Appl. Catal., A* **2010**, *390*, 71–77.
(41) Grossale, A.; Nova, I.; Tronconi, E. *Catal. Today* **2008**, *136*, 18–27.
(42) Grossale, A.; Nova, I.; Tronconi, E. *Catal. Lett.* **2009**, *130* 525–531.
(43) Delahay, G.; Valade, D.; Guzmán-Vargas, A.; Coq, B. *Appl. Catal., B* **2005**, *55*, 149–155.
(44) Huang, H. Y.; Long, R. Q.; Yang, R. T. *Appl. Catal., A* **2002**, *235* 241–251.
(45) Metkar, P. S.; Salazar, N.; Muncrief, R.; Balakotaiah, V.; Harold, M. P. *Appl. Catal., B* **2011**, *104*, 110–126.
(46) Kröcher, O.; Devadas, M.; Elsener, M.; Wokaun, A.; Soger, N.; Pfeifer, M.; Demel, Y.; Mussmann, L. *Appl. Catal., B* **2006**, *66*, 208–216.
(47) Giles, R.; Cant, N. W.; Kogel, M.; Turek, T.; Trimm, D. L. *Appl. Catal., B* **2000**, *25*, L75–L81.
(48) Brüggemann, T. C.; Keil, F. J. *J. Phys. Chem. C* **2011**, *115*, 2114–2133.
(49) Schuler, A.; Drochner, A.; Vogel, H.; Malmberg, S.; Votsmeier, M.; Gieshoff, J.; Söger, N.; Mußmann, L. *Chem. Ing. Tech.* **2006**, *78*, 1246.
(50) Grossale, A.; Nova, I.; Tronconi, E. *J. Catal.* **2009**, *265*, 141–147.
(51) Devadas, M.; Kröcher, O.; Elsener, M.; Wokaun, A.; Mitrikas, G.; Soger, N.; Pfeifer, M.; Demel, Y.; Mussmann, L. *Catal. Today* **2007**, *119*, 137–144.
(52) Iwasaki, M.; Yamazaki, K.; Shinjoh, H. *Appl. Catal., A* **2009**, *366*, 84–92.
(53) Forzatti, P.; Nova, I.; Tronconi, E. *Angew. Chem., Int. Ed.* **2009**, *48*, 8366–8368.
(54) Forzatti, P.; Nova, I.; Tronconi, E. *Ind. Eng. Chem. Res.* **2010**, *49*, 10386–10391.
(55) Long, R. Q.; Yang, R. T. *Chem. Commun.* **2000**, 1651–1652.
(56) Akah, A.; Cundy, C.; Garforth, A. *Appl. Catal., B* **2005**, *59*, 221–226.
(57) Akah, A. C.; Nkeng, G.; Garforth, A. A. *Appl. Catal., B* **2007**, *74*, 34–39.
(58) Long, R. Q.; Yang, R. T. *J. Catal.* **2001**, *201*, 145–152.
(59) Qi, G. S.; Gatt, J. E.; Yang, R. T. *J. Catal.* **2004**, *226*, 120–128.
(60) Qi, G. S.; Yang, R. T. *Appl. Catal., A* **2005**, *287*, 25–33.
(61) Heyden, A.; Peters, B.; Bell, A. T.; Keil, F. J. *J. Phys. Chem. B* **2005**, *109*, 1857–1873.
(62) Heyden, A.; Hansen, N.; Bell, A. T.; Keil, F. J. *J. Phys. Chem. B* **2006**, *110*, 17096–17114.
(63) Hansen, N.; Heyden, A.; Bell, A. T.; Keil, F. J. *J. Phys. Chem. C* **2007**, *111*, 2092–2101.
(64) Coq, B.; Mauvezin, M.; Delahay, G.; Kieger, S. *J. Catal.* **2000**, *195*, 298–303.
(65) Guzmán-Vargas, A.; Delahay, G.; Coq, B. *Appl. Catal., B* **2003**, *42*, 369–379.
(66) Coq, B.; Mauvezin, M.; Delahay, G.; Butet, J.-B.; Kieger, S. *Appl. Catal., B* **2000**, *27*, 193–198.
(67) Delahay, G.; Mauvezin, M.; Coq, B.; Kieger, S. *J. Catal.* **2001**, *202*, 156–162.
(68) Ates, A. *Appl. Catal., B* **2007**, *76*, 282–290.
(69) Sugawara, K.; Nobukawa, T.; Yoshida, M.; Sato, Y.; Okumura, K.; Tomishige, K.; Kunimori, K. *Appl. Catal., B* **2007**, *69*, 154–163.
(70) Nova, I.; Ciardelli, C.; Tronconi, E.; Chatterjee, D.; Weibel, M. *Top. Catal.* **2007**, *42−43*, 43–46.
(71) Grossale, A.; Nova, I.; Tronconi, E.; Chatterjee, D.; Weibel, M. *J. Catal.* **2008**, *256*, 312–322.
(72) Koebel, M.; Elsener, M.; Madia, G. *Ind. Eng. Chem. Res.* **2001**, *40*, 52–59.
(73) Koebel, M.; Madia, G.; Elsener, M. *Catal. Today* **2002**, *73*, 239–247.
(74) Yeom, Y.; Henao, J.; Li, M.; Sachtler, W.; Weitz, E. *J. Catal.* **2005**, *231*, 181–193.
(75) Savara, A.; Sachtler, W. M.; Weitz, E. *Appl. Catal., B* **2009**, *90*, 120–125.
(76) Li, J.; Li, S. *J. Phys. Chem. C* **2008**, *112*, 16938–16944.
(77) Schwidder, M.; Kumar, M. S.; Brückner, A.; Grünert, W. *Chem. Commun.* **2005**, 805.
(78) Brüggemann, T. C.; Keil, F. J. *J. Phys. Chem. C* **2009**, *113*, 13860–13876.
(79) Brüggemann, T. C.; Vlachos, D. G.; Keil, F. J. *J. Catal.* **2011**, *283*, 178–191.
(80) Olson, D. H.; Kokotailo, G. T.; Lawton, S. L.; Meier, W. M. *J. Phys. Chem.* **1981**, *85*, 2238–2243.
(81) Ahlrichs, R.; Bär, M.; Haser, M.; Horn, H.; Kolmel, C. *Chem. Phys. Lett.* **1989**, *162*, 165–169.
(82) Treutler, O.; Ahlrichs, R. *J. Chem. Phys.* **1995**, *102*, 346.
(83) Peters, B.; Heyden, A.; Bell, A. T.; Chakraborty, A. *J. Chem. Phys.* **2004**, *120*, 7877.
(84) Heyden, A.; Bell, A. T.; Keil, F. J. *J. Chem. Phys.* **2005**, *123*, 224101.
(85) Baker, J. *J. Comput. Chem.* **1986**, *7*, 385–395.
(86) Zilberberg, I.; Gora, R. W.; Zhidomirov, G. M.; Leszczynski, J. *J. Chem. Phys.* **2002**, *117*, 7153.
(87) RadonÌĄ, M.; Broclawik, E.; Pierloot, K. *J. Phys. Chem. B* **2010**, *114*, 1518–1528.
(88) Chen, H.; Song, J.; Lai, W.; Wu, W.; Shaik, S. *J. Chem. Theory Comput.* **2010**, *6*, 940–953.
(89) Harvey, J. N.; Aschi, M. *Phys. Chem. Chem. Phys.* **1999**, *1*, 5555–5563.
(90) Zhao, Y.; González-García, N.; Truhlar, D. G. *J. Phys. Chem. A* **2005**, *109*, 2012–2018.
(91) Sousa, S. F.; Fernandes, P. A.; Ramos, M. J. *J. Phys. Chem. A* **2007**, *111*, 10439–10452.
(92) Harvey, J. N. *Phys. Chem. Chem. Phys.* **2007**, *9*, 331–343.
(93) Guesmi, H.; Berthomieu, D.; Kiwi-Minsker, L. *J. Phys. Chem. C* **2008**, *112*, 20319–20328.
(94) Hansen, N.; Heyden, A.; Bell, A. T.; Keil, F. J. *J. Catal.* **2007**, *248*, 213–225.
(95) Heyden, A.; Bell, A.; Keil, F. *J. Catal.* **2005**, *233*, 26–35.

(96) Guesmi, H.; Berthomieu, D.; Bromley, B.; Coq, B.; Kiwi-Minsker, L. *Phys. Chem. Chem. Phys.* **2010**, *12*, 2873.
(97) Heyden, A. Theoretical investigation of the nitrous oxide decomposition over iron zeolite catalysts. *Ph.D. Thesis*, TUHH; 2005.
(98) Chatterjee, D.; Kočí, P.; Schmeißer, V.; Marek, M.; Weibel, M.; Krutzsch, B. *Catal. Today* **2010**, *151*, 395–409.
(99) Long, R. Q.; Yang, R. T. *J. Catal.* **1999**, *188*, 332–339.